construction
engineering
research
laboratory

United States Army
Corps of Engineers
...Serving the Army
...Serving the Nation

TECHNICAL REPORT N-13
November 1976
Prediction and Reduction of the Noise Impact Within
and Adjacent to Army Facilities

THE STATISTICS OF AMPLITUDE AND SPECTRUM OF BLASTS PROPAGATED IN THE ATMOSPHERE

VOLUME I

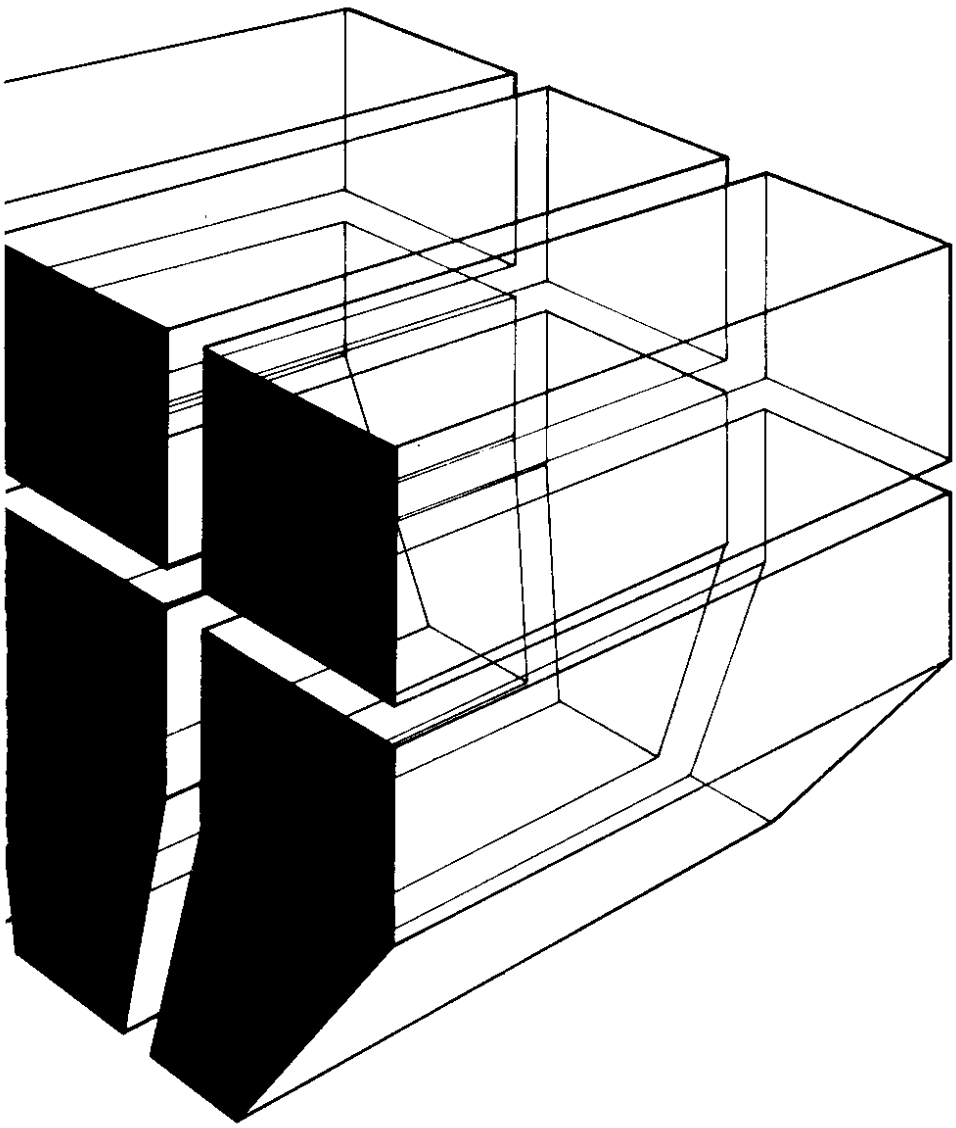

by
P. D. Schomer
R. J. Goff
L. M. Little

Foreword

This research was conducted for the Directorate of Military Construction, Office of the Chief of Engineers (OCE), under Project 4A162121A896, "Environmental Quality for Army Construction"; Task 06, "Noise Pollution Control"; Work Unit 001, "Prediction and Reduction of the Noise Impact Within and Adjacent to Army Facilities." The applicable QCR is 1.03.011. Mr. Frank Beck served as the OCE Technical Monitor.

This work was performed by the Acoustics Team (Dr. P. D. Schomer, Chief) of the Environmental Division (Dr. R. K. Jain, Chief), U. S. Army Construction Engineering Research Laboratory (CERL).

The Federal Aviation Administration, the Army Environmental Hygiene Agency, and D Company of the 5th Engineering Battalion, Fort Leonard Wood, MO, are acknowledged for their assistance in gathering pertinent data.

COL J. E. Hays is Commander and Director of CERL, and Dr. L. R. Shaffer is Deputy Director.

Contents

List of Figures and Tables

Figures

Tables

1 Introduction

Background

In a continuing study, the U.S. Army Construction Engineering Research Laboratory (CERL) is developing a methodology for predicting and assessing the noise impact of a military facility's operations. A number of noise sources have been identified, including blasts, rotary-wing and fixed-wing aircraft, and vehicular and fixed sources. On the basis of priority of importance, blast noise and rotary-wing aircraft were selected as the Army's major noise problems.

In order to resolve the problem of blast noise prediction, a variety of research projects has been undertaken. In CERL Report E-17,[1] an initial blast noise prediction model was developed using data existing in 1971. This report consisted of two parts: (1) a method for calculating blast amplitudes on the basis of distance, source characteristics, and meteorological conditions, and (2) a method for using these amplitudes to predict the probable community response.

As a continuation of this research, a computer program implementing the model was written. Using data sheets[2] on which military facilities supplied such information as location of firing points and impact areas, number of firings per day, size of charges, time of day, and types of weapons, the program calculated Noise Exposure Forecast (NEF) contours over a grid of points on and surrounding the military facility.[*] These contours were then used to evaluate the community response so that corrective steps could be taken in problem areas.

---

[1] P. D. Schomer, *Predicting Community Response to Blast Noise,* Technical Report E-17/AD773690 (U.S. Army Construction Engineering Research Laboratory [CERL], 1973).

[2] B. Homans, J. McBryan, and P. Schomer, *User Manual for the Acquisition and Evaluation of Operational Blast Noise Data,* Technical Report E-42/AD782911 (CERL, 1974).

* NEF contours were initially used to estimate community response to aircraft noise and to establish zones of relative acceptability. The rating considers the amplitude and frequency characteristics in a manner that closely matches human judgment of the event's noisiness. Duration and time of occurrence are also considered.

The original blast noise prediction model contained a number of data deficiencies; the two most significant were the statistics of blast propagation in the atmosphere and the relationship of human response to blast stimuli. Two studies were initiated to provide these data. One study, being conducted at Stanford Research Institute, is designed to quantify human response to blast stimuli. The second study was initiated to quantify blast propagation statistics by taking detailed blast noise measurements at a number of sites. This report covers measurements made at one of the sites — Fort Leonard Wood, MO.

Purpose

The purposes of this report are (1) to develop the blast propagation statistics of the measured data, (2) to relate these results to specific meteorological and terrain conditions at Fort Leonard Wood, and (3) to develop frequency-weighted one-third octave spectra of blast amplitudes for use in predicting human response to blast stimuli.

Approach

Quantifying blast propagation statistics requires a two-step approach. The first step is the development of these statistics in relation to a specific set of meteorological and terrain conditions. The second is the translation of these results to other geographic areas.

Step 1 can be accomplished with the data obtained from Fort Leonard Wood, MO, the first in a planned series of sites. Being centrally located in the midwest, its climate is typical of a large portion of the country. From statistical analysis, any existing relationships can be determined between measured amplitudes and other various parameters. Step 2, however, is more difficult. The detection of terrain effects is not always possible because prevailing winds and other weather effects may dominate. Moreover, while the translation of statistics from one part of the country to another (based upon readily available site-specific meteorological and terrain attributes) can be inferred from one set of data, in reality it requires measurements at a number of locations to verify relationships. Consequently, this step will be carried out in subsequent studies through the translation of the Fort Leonard Wood statistics to other geographic areas of the United States. Nonetheless, these two steps both formed a basis for defining the experimental plan of this initial report.

Over 700 5-lb (2 kg) charges of C4 explosives were detonated over a relatively flat and open area. By keeping the source constant, the statistics of the received signal could be developed as a function of distance, terrain, and meteorological conditions. Simultaneous wide-band analog recordings were made of these blasts at 16 stations located at distances of 2, 5, 10, and 15 mi (3, 8, 16, and 25 km) and in four directions (north, east, south, and west).* In addition, peak values of the blast amplitudes were measured to insure that the analog recordings would not be overloaded and to provide results that could be related to earlier studies.**

From these wide-band analog recordings, various weighted and unweighted frequency spectra were developed for use in predicting community response. Also determined was a frequency-weighted integral of the time history of the pressure squared, a quantity termed Sound Exposure Level or SEL. In addition, these recordings formed a general data base from which the propagation statistics and resulting noise impact could be described.

To obtain a base of meteorological data, measurements of wind speed, wind direction, temperature, humidity, and turbulence were required at different altitudes. Ideally, these conditions should be defined at all points in space of the area of interest at the time of propagation; however, military facilities have limited meteorological data available, and obtaining such extensive information would be impractical. A weather plane or balloon making measurements takes substantial time to climb from ground level to upper altitudes. Moreover, the data obtained will be a function of altitude only at one area, while in reality inversion heights, wind, and other functions change as a function of position over the ground. Nonetheless, it was decided to gather as much site-specific meteorological data as possible for use in developing relations with the blast amplitudes. Since this weather data is still more detailed than that usually available, it can be used to confirm relationships that have previously only been implied. These measurements were obtained with the use of FAA equipment, manpower, and aircraft.

---

* Measurements were also made at distances of 1000, 2000, and 5000 ft (301, 602, and 1506 m) in these four directions. These analyses will be the subject of a subsequent report.

** Since the peak value is not directly related to human sensitivity, it is not used to predict community response to blast noise. For example, although a child's cap pistol fired near a building and an artillery round detonated several miles away produce the same peak amplitude at the wall of the building, the artillery round, which contains more energy and lasts longer, will shake the building and cause complaints, while the cap pistol will not.

Organization of Report

Chapter 2 describes the procedures and measurements used in gathering the acoustical and meteorological data; Chapter 3 contains the reduction and analysis of these data.

Chapters 4 through 7 establish relationships between the acoustic signal and such parameters as distance, terrain, and meteorological conditions. Analysis is performed on both an individual blast basis and a statistical basis.

Chapter 8 summarizes the results, and the appendices provide detailed data. Appendices A (raw sound velocity profile data) and B (details of amplitude distribution) are in this volume. Appendices C (one-third octave spectra), D (absolute, relative, and difference energy-average octave spectra), and E (difference distributions) are bound separately as Volume II.

2 Collection of Data

An array of measurement stations was set up to obtain the data necessary for the development of blast propagation statistics (Figure 1). When a blast was detonated in the target area, simultaneous analog recordings were made in four directions at distances of 2, 5, 10, and 15 mi (3, 8, 16, and 24 km). Concurrent with these measurements, an FAA plane flew ascending and descending patterns over the test area to record wind speed, wind direction, temperature, humidity, and turbulence. This chapter details these acoustic and meteorological measurements.

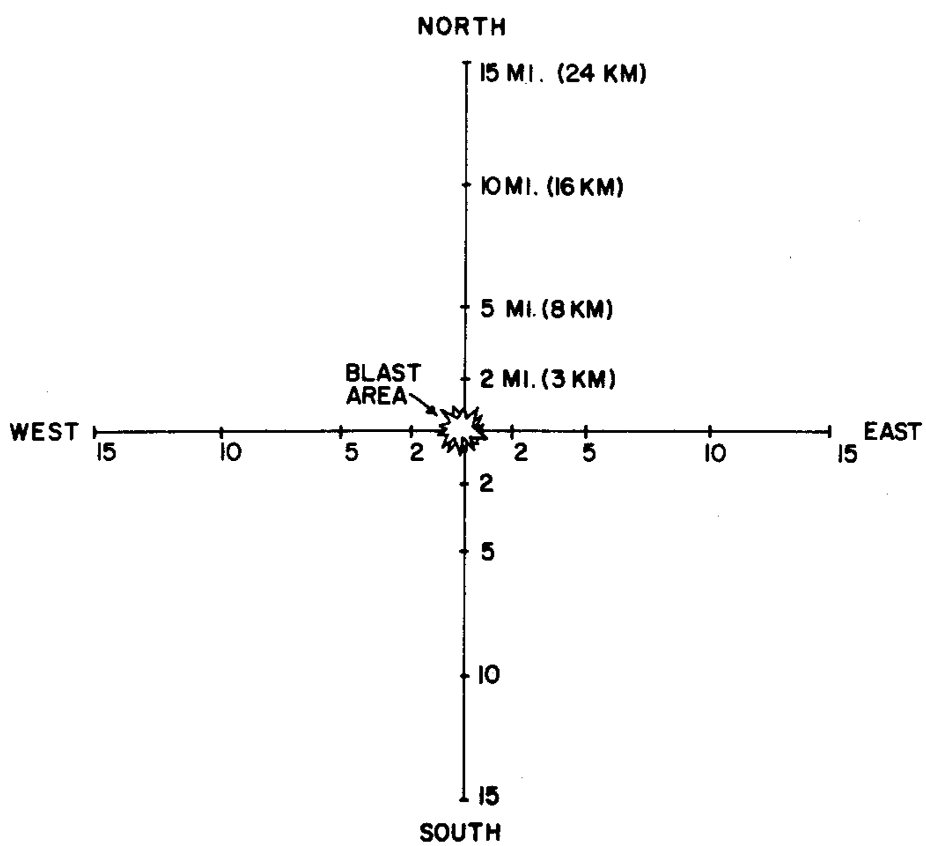

Figure 1. Array of measurement stations.

Acoustic Measurements

Fort Leonard Wood is located in the Missouri Ozarks. Although the land is generally hilly and densely forested, most measurement stations were placed on relatively high ground in open areas. The measurements were taken in late spring 1973. On a typical sunny day, the nighttime ground level inversions began to rise and dissipate approximately 2 to 3 hours after sunrise. Later, as the temperature rose, the temperature gradient became more negative.

To include as many varied weather conditions as possible, measurements began at dawn (0500 hours) and continued until 1100 hours; after 1100 hours, the weather remained constant throughout the day. Because the FAA plane could not make ground passes at night, measurements could not occur earlier than 0500 hours.

The measurement stations, manned by specially trained engineer troops from D Company of the 5th Engineer Battalion, were dividing into five groups (Table 1).

Table 1. Measurement station groups.

Group	Direction	Distance from Target
1	North	5,10, and 15 mi (8, 16, and 24 km)
2	South	5,10, and 15 mi (8, 16, and 24 km)
3	East	5,10, and 15 mi (8, 16, and 24 km)
4	West	5,10, and 15 mi (8, 16, and 24 km)
5	All	2 mi (3 km)

The stations in each group were coordinated by a CERL technical supervisor who periodically monitored the equipment at each location. Use of these troops enabled researchers to use four-wheel drive vehicles for reaching measurement locations and VHF radios for communications.

The basic equipment at these stations included: (1) a B&K 4145 microphone; (2) a B&K 2209 or 2204 impulse sound level meter; (3) a Nagra DJ or SJ tape recorder; (4) a Nagra QC-JA attenuator for connecting sound level meter AC output to tape recorder input; (5) a voice microphone for commentary data; (6) a wind screen, tripod, and 33-ft (10 m) microphone extension cable; (7) batteries for tape recorder and a power cable for 24-V vehicle battery; (8) clipboards, pens, and data logs; (9) spare batteries; (10) a PRC-77, VRC-46, or 47 VHF radio; and (11) compartmented cases for holding and storing the field station equipment. Figure 2 is a block diagram of a typical equipment setup.*

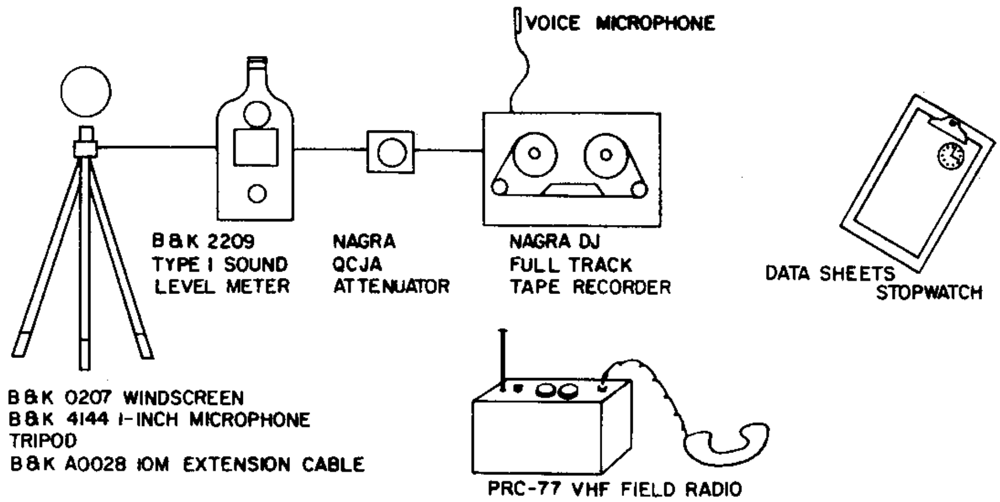

Figure 2. Equipment setup for a distant manned field station.

For stations in Groups 1 through 4, a B&K 4145 1-in. (25 mm) microphone was placed on a tripod approximately 4 1/2 ft (1.4 m) above the ground and covered with a polyurethane foam windscreen. A B&K AO-0028 33-ft (10 m) cable connected the microphone to a B&K 2209 sound level meter which, coupled to a Nagra DJ tape recorder, acted as a preamplifier. The sound level meter was set on its linear weighted peak hold response for visual analysis. The tape recorders were adjusted so that signals 7 dB above full scale (plus 10 dB) on the sound level meter would read 0 dB on the recorder VU-meter. Recordings were made at 1.5 in./sec (3.8 cm/sec) while subsequent analyses were made at 15 in./sec (38.1 cm/sec).

With this procedure, the effective low frequency of the tape recorders was 2 Hz, which could allow wind noise to interfere with the blast signal. To eliminate this problem, the 10-Hz cutoff on the sound level meter was usually employed. Since the microphone and recorder could operate down to 2 Hz, and the internal elec-

---

* In a separate test, CERL personnel compared the results from these manned stations to those obtained from an FM microphone feeding into an FM recorder. The measured peak levels were the same for both systems as well as the spectral content in the range of 10 Hz to 2 kHz or 3.5 kHz with the Nagra SJ Recorder (the signal contained no energy above 2 kHz). The manned stations lost low-frequency phase information below 10 Hz, but these data are not significant in predicting community noise impact.

tronics of the sound level meter were capable of detecting 0.1 Hz, the simple pole at 10 Hz defined the low-frequency characteristics of the measurement system.

At the 2-mi (3 km) stations (Group 5), B&K 2204 sound level meters were used in conjunction with Nagra SJ recorders instead of the B&K 2209 sound level meter and Nagra DJ recorder combination. Since high frequencies were most likely to occur close to the source, the Nagra SJ recorder with its upper frequency limit of 3.5 kHz was more accurate than the DJ recorder with its 2.0 kHz limit. Because the B&K 2204 sound level meter could not be monitored during recording, the equipment operators monitored the VU-meter of the Nagra SJ recorder, which was equipped with a quasi-peak-response position.

The CERL technical supervisor at each station performed normal pistonphone calibration of the sound level meters at the beginning and end of each day and two or three additional times throughout the day. The calibration signal was also recorded by the Nagra tape recorder. This RMS calibration signal, which created a plus 4-dB deflection on the sound level meter, registered about minus 3 on the tape recorder VU-meter with the gain on the sound level meter lowered by 10 dB.

Wide-band frequency response tests were made on all equipment before the field measurements (by the manufacturers) and after its return to CERL (by CERL personnel).

Once the equipment was set up and calibrated, the following sequence was used to record the blast noise:

1. When the fuse for the 5-lb (2 kg) C-4 charge was lit, the Communication Officer informed the equipment operators by radio, “Test number 57 (hypothetical number) coming.”
2. Approximately 45 sec after the first radio call, the equipment operators were told “Test number 57, turn on recorders, test number 57.”
3. The operators turned on their recorders, said “Test number 57” into the voice microphones, and left the recorders running.
4. When the blast occurred, the command “mark” was given over the radio; the equipment operators responded by saying “mark” into the voice microphone and turning its gain control fully down.
5. The recorders were operated somewhat longer than the travel time of sound from the blast site to the recording location. Depending on the distance from the blast site — 2, 5, 10, or 15 mi (3, 8, 16, or 24 km) the operators turned off the recorder after 20, 35, 65, or 105 sec, respectively. The blast amplitudes were also recorded on the peak hold position of the sound level meter.

6. The equipment operators then read the sound level meter and recorded the reading, the blast number, and meter attenuator setting in the data log. Because of this very simple procedure — the only control moved by the equipment operators was the outer 10-dB attenuator switch on the sound level meters — virtually no difficulties were experienced with operation of the equipment.
7. The procedure was repeated for each blast.*

As expected, not all stations were able to operate all of the time. Early morning fog, communication or mechanical breakdowns, and moisture on microphones occasionally prevented operation at certain locations. Also, measurements were not usually performed in the rain.

Meteorological Measurements

During the testing between 0500 and 1100 hours, an FAA plane made repeated ascents over the entire test area to gather weather data. Wind speed and direction were measured at 1000, 2000, and 3000 ft (204, 610, and 914 m) above ground level (AGL), while temperatures were obtained for altitudes between 0 and 3000 ft (914 m) AGL. Weather-sensing probes mounted on the body of the plane fed information to recorders inside the cabin. A technician inside the plane also manually recorded altitude and temperature. Wind speed and direction were measured only during level flight, which was maintained with navigational aid from the nearby airport. Hourly ground conditions were taken from the airport meteorological units.

After the required acoustical and meteorological data were collected using this methodology, they were put in a format applicable to the analytical procedures in Chapter 3.

---

* Throughout the entire measurement process, communications were a primary logistic requirement. Five channels were employed to establish contact between the control site and the actual blast site (to oversee the lighting of fuses), the base switchboard, the manned stations in Groups 1 to 5, the FAA plane (to coordinate the detonation with the aircraft flight), and the close-in unmanned stations.

3 Data Analysis

Two sets of data were obtained using the procedures in Chapter 2. The meteorological data included wind speed, wind direction, and temperature according to altitude, while the blast data consisted of tape recordings of detonations at various distances. Each set required separate analysis before the sets could be combined to establish a statistical relationship.

Analysis of Meteorological Data

To analyze the meteorological data, a computer program first separated the wind velocity into north, east, south, and west components. It then plotted sound velocity profiles or gradients as a function of altitude, using Eq 1:[3]

$$C = 331.6\sqrt{1 + T/273} + Vw \quad \text{[Eq 1]}$$

where C = velocity of sound in m/sec

Vw = wind velocity in m/sec

T = air temperature in °C.

Figure 3 presents raw sound velocity profile data produced by the computer from information obtained by the FAA plane. Breakpoints and slopes were chosen from this raw data to create the sound velocity profile in Figure 4.

Each profile contained at least three slopes representing either positive or negative gradients. Thus, the profiles could be characterized as negative-positive-negative, positive-positive-positive, etc. A separate profile was computed for each direction for each weather run. Appendix A presents the profile data.

[3] R. S. Thompson, *Computing Sound Ray Paths in the Presence of Wind*, Report SC-RR-67-53 (Sandia Laboratories, 1967), p 7.

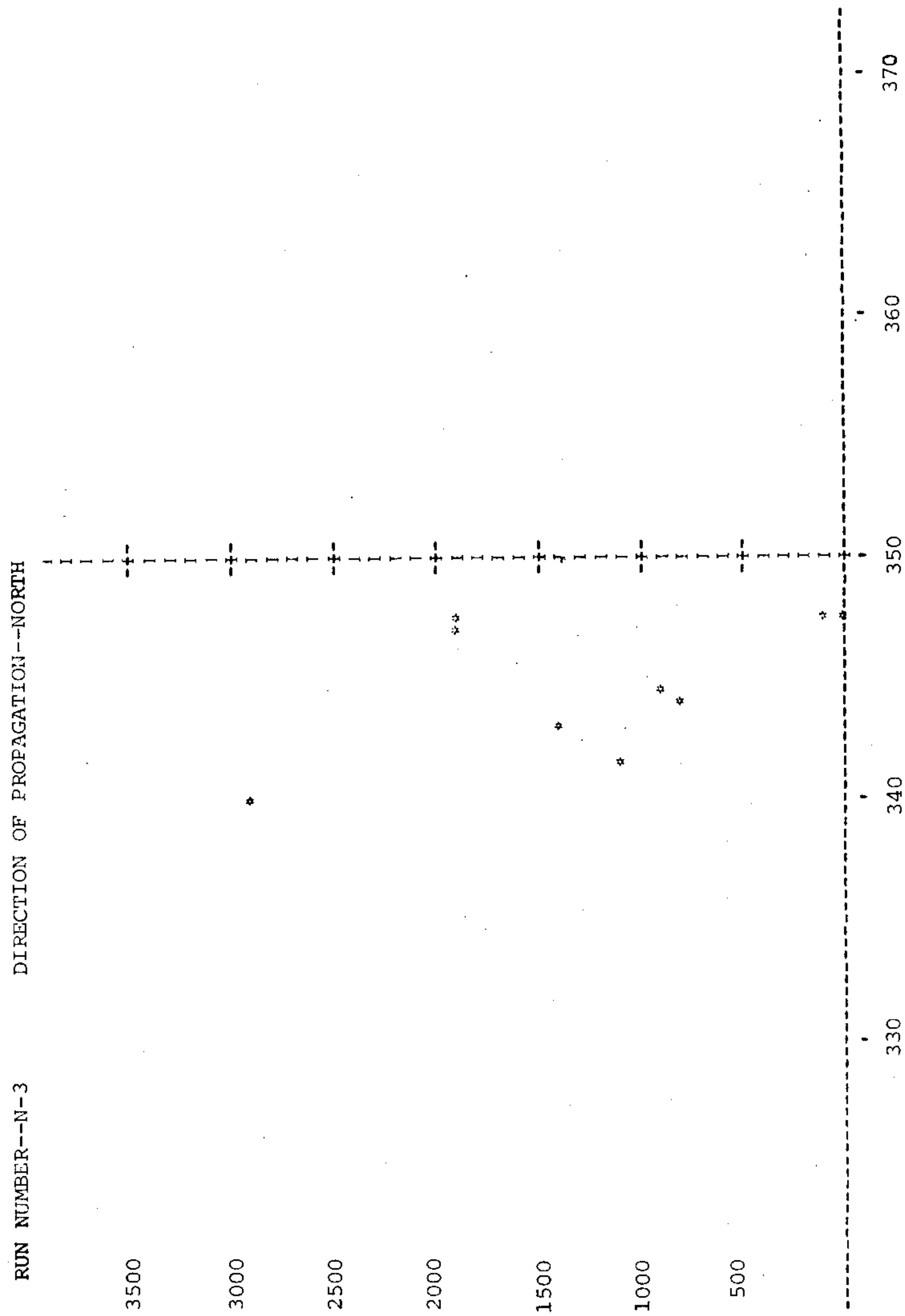

Figure 3. Computer-generated raw sound velocity profile data.

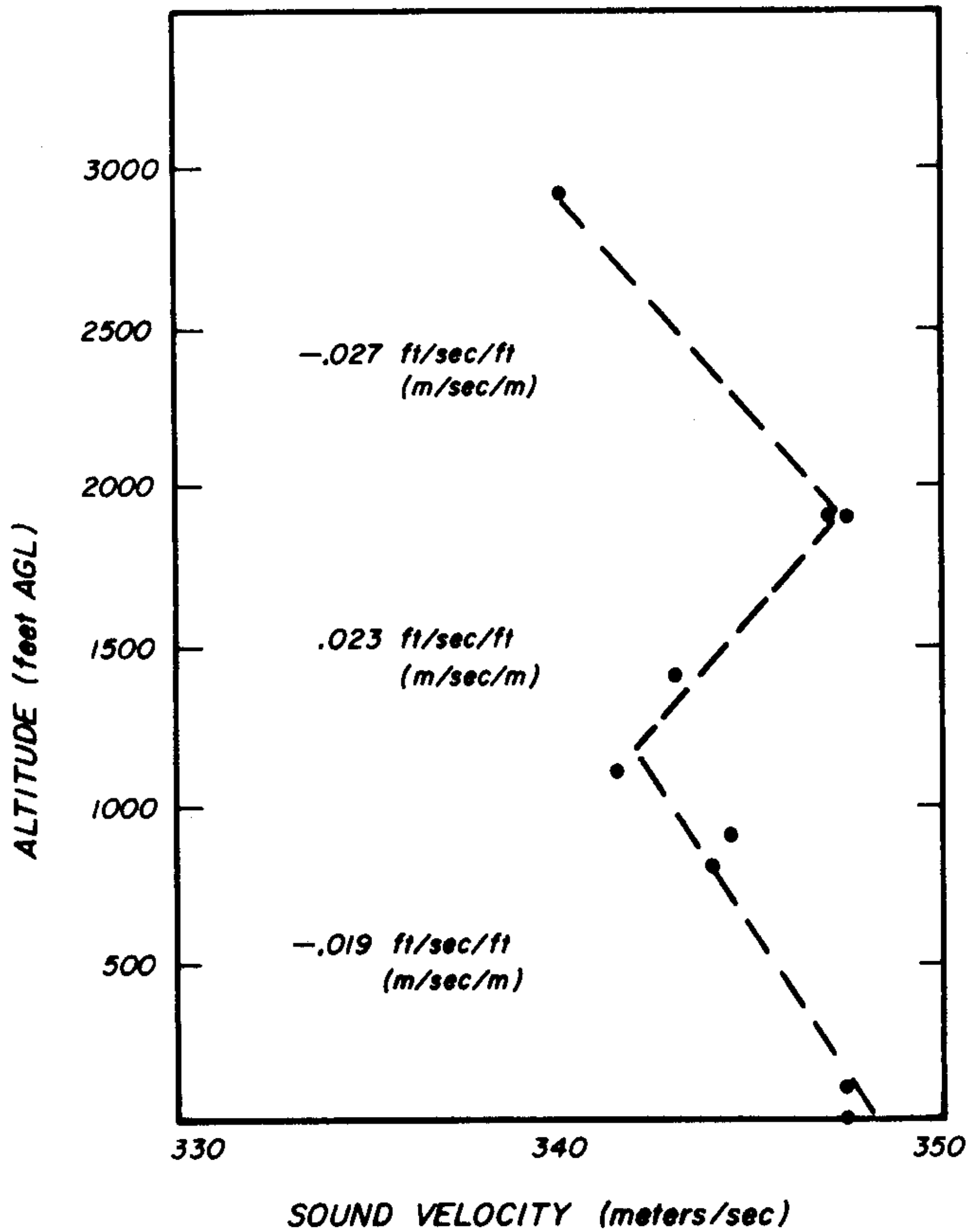

Figure 4. Sound velocity gradient profile with breakpoints and slopes.

Analysis of Blast Data

The blast data analysis consisted of determining the peak value and frequency spectra of each blast and required reduction of the acoustical signatures on the magnetic tape. By relating these signatures to the attenuator setting of the sound level meter and the recorded calibration signals, sound pressure levels were established for all blast transients. The peak levels were later rechecked with the visual observations made in the field. Individual frequency spectra were obtained from a narrow-band analysis performed by a Federal Scientific UA-14A 400 Line Analyzer.*

Figure 5 illustrates the analysis procedure. The recorded blast signals were played into the transient mode of the 400 line analyzer. Two minitor oscillis-copes were then employed; one to display the contents of the analyzer memory to insure that the recorded blast transient was a clean signal uncorrupted by noise or otherwise distorted, and the second to display the narrow-band spectrum. The analyzer itself was directly interfaced to a computer that summed the spectral lines to form one-third octaves. Along with normalizing and gain-correcting information, these data were then stored on magnetic discs for subsequent analysis, which included calculation of frequency-weighted measures and statistics for the stored data.

To test the validity of obtaining one-third octaves from a narrow-band analysis, the spectra were compared to two separate sets of one-third octave spectra obtained from the procedure outlined in Figure 6. The recorded blasts were played through a B&K 7502 transient recorder into a sound level meter via a one-third octave filter. An “impulse spectrum” was obtained by playing the transient signal through each filter once and reading the results in the impulse hold position of the sound level meter. A “steady-state spectrum” was obtained by repeatedly playing the signal through each filter to establish a steady-state condition, and then reading the results using slow meter response of the sound level meter.

* Conceptually, analyzing a transient requires that the signal be played repeatedly through a set of filters. A loop of tape can facilitate analysis and also eliminate the need to read maximum instantaneous values. The UA-14A Line Analyzer automatically forms a loop from the data and measures narrow-band spectra in real time as if it were a parallel narrow-band 400-element filter set.

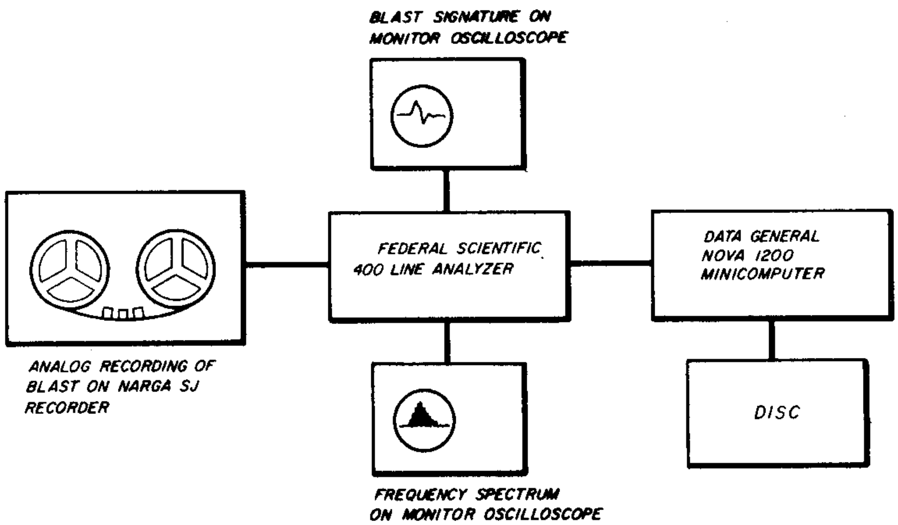

Figure 5. Schematic of narrow-band spectral analysis.

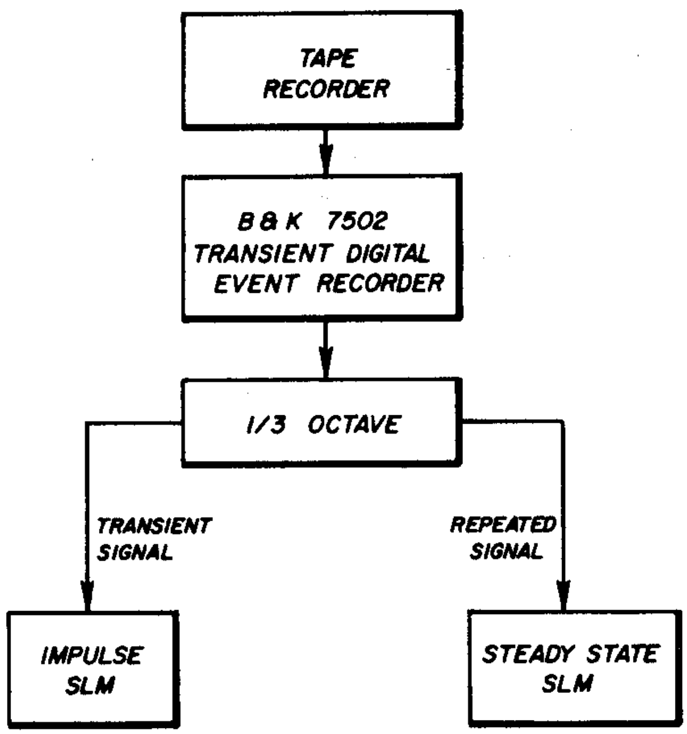

Figure 6. Schematic of impulse and steady-state one-third octave spectral analysis.

Comparisons of the one-third octave spectra from the 400 line analyzer with the impulse spectra and the steady-state spectra are shown in Figures 7 and 8, respectively. Although the figures indicate near-perfect agreement, one-third octaves produced by the 400 line analyzer (with its sharp filter skirts) have deeper dips than those produced by the one-third octave filter (with shallower filter skirts), as expected.

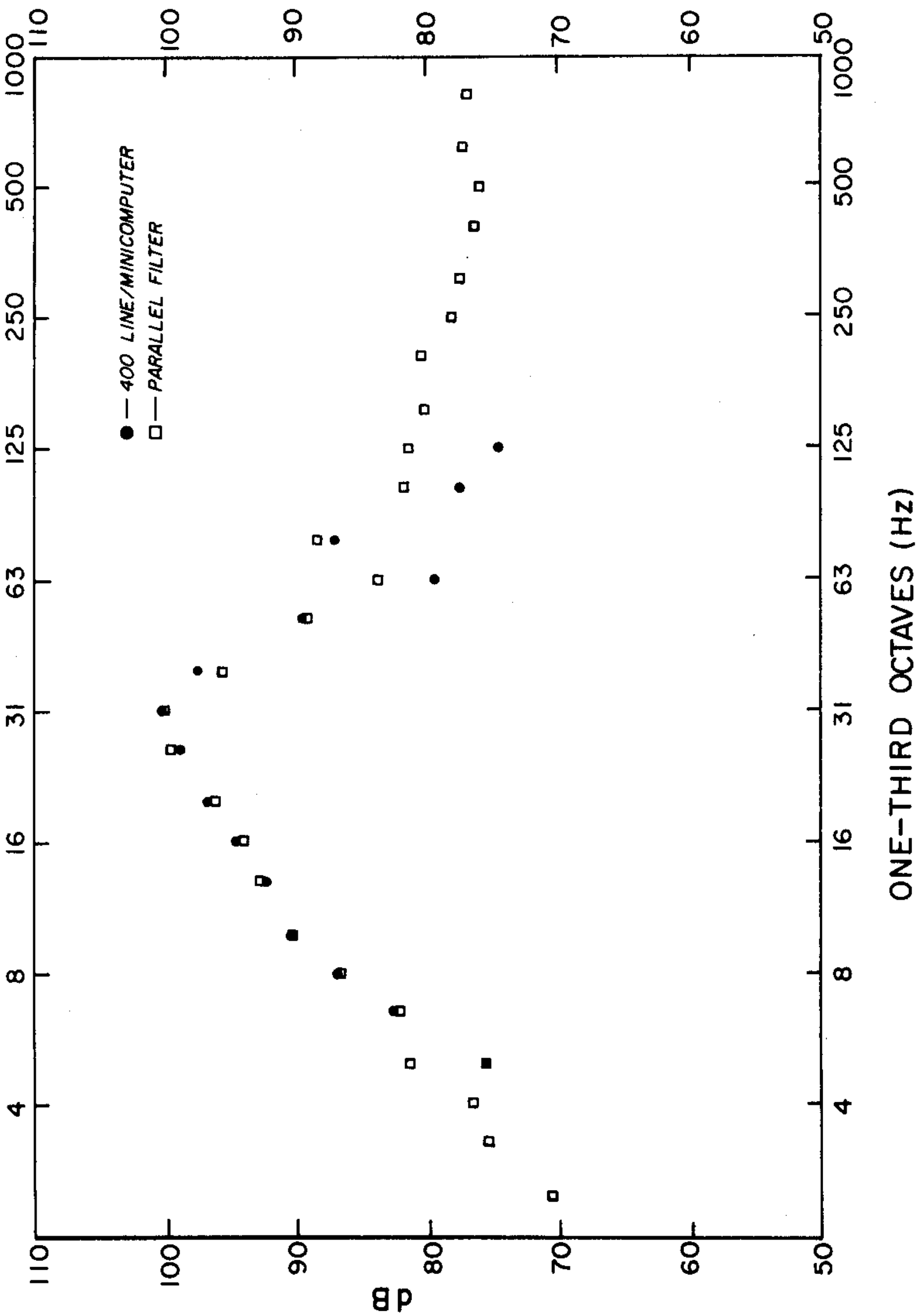

Figure 7. Comparison of 400 line analyzer spectra with impulse spectra.

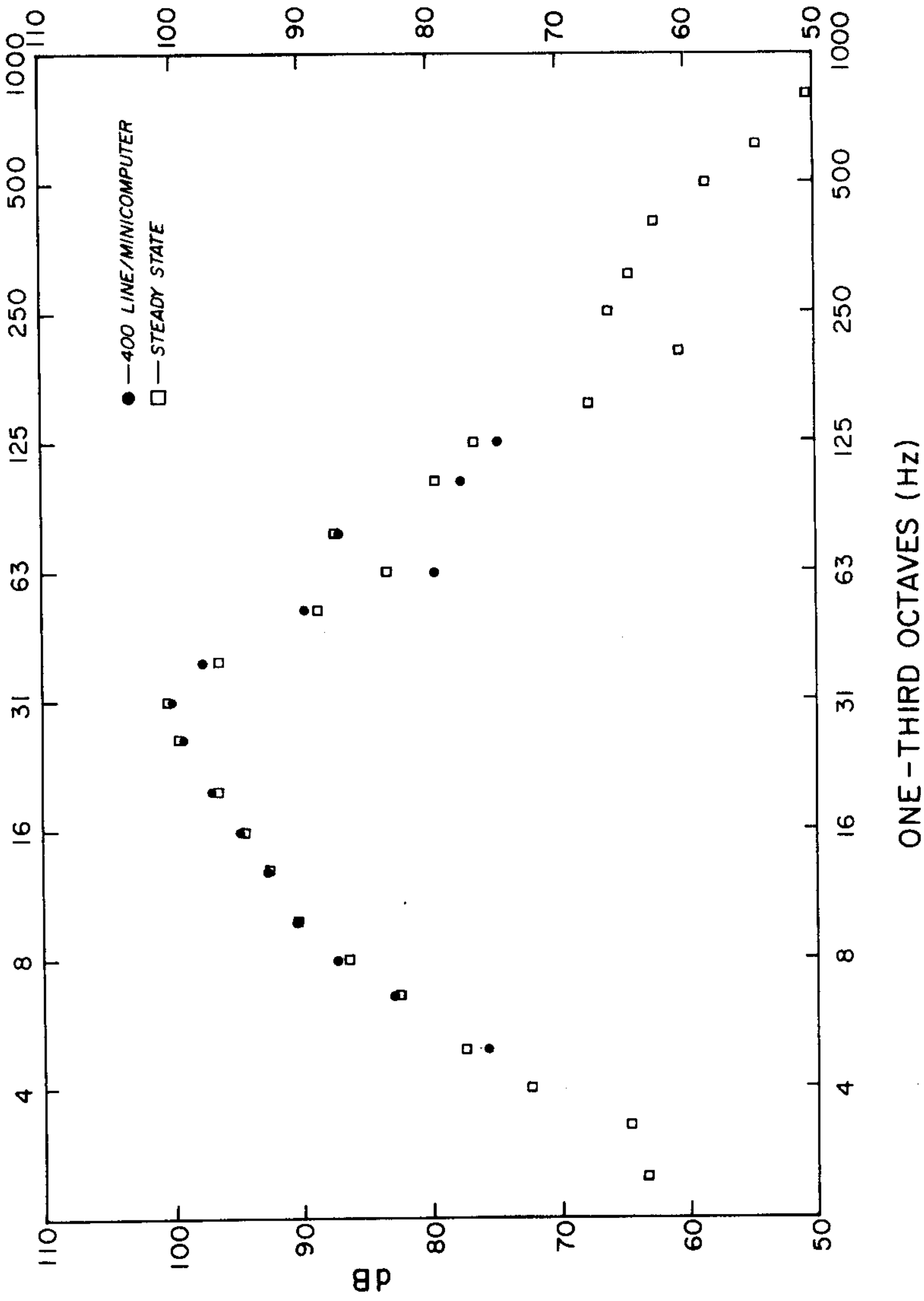

Figure 8. Comparison of 400 line analyzer spectra with steady-state spectra.

While this comparison verified relative spectrum shapes, it did not determine absolute levels. This calculation required use of the recorded calibration tone, which could not be used directly with the 400 line analyzer because of a discrepancy between continuous signals which completely fill its memory and transient blast signals which only fill its memory to 70 to 80 percent capacity. Consequently, another approach was used for each blast. Since the entire acoustic signature was essentially stored in the memory (1-sec duration) of the 400 line analyzer, the analysis time period included all of the significant signal. Consequently, the spectral output was a true Fourier analysis of the time-varying signal.

It is a basic theorem of Fourier theory that the integral of the squared spectrum over frequency is equal to the integral of the squared time-varying original signal (in this case, pressure, p) over all time, T. Thus, by determining the value for the integral of the time-varying signal squared — $\int p^2(t)dt$ — the absolute value of these spectra could be obtained using the following relationship from Fourier analysis:

$$\frac{1}{p_0^2}\int_{-\infty}^{\infty} p^2(t)dt = \frac{1}{p_0^2}\int_0^t p^2(t)dt = \sum_{i=1}^{43} 10^{L_i/10} \qquad \text{[Eq 2]}$$

where p_0 = .0002 microbar

t = 1 sec

L_i = 1 /3 octave band level (dB) for the i^{th} band as determined by narrow-band analysis.

Two methods were used to calculate this pressure-squared integral. In one method, the recorded blast signatures and calibration tones for approximately 20 percent of the data were digitized using a 4-kHz sampling rate on a B&K 7502 transient digital event recorder. The resulting information was squared and summed on a Wang 600 computing calculator to get a true absolute value. In the second method, the same tapes were played into two sound level meters simultaneously. One meter was set on impulse hold, while the second was set on peak hold. Figure 9 compares these impulse and peak values to the pressure-squared integrals from the digital event recorder and shows the definite relationship that was established.*

$$\text{Impulse level} - \int p^2(t)dt = \text{Function of peak amplitude.}$$

From Figure 9 and the impulsive and peak amplitude readings, a good approximation of the pressure-squared integral was obtained for the remaining 80 percent of the blast data without using the lengthy process of digitizing. These numbers were then used as the absolute values for the one-third spectra obtained with the 400 line analyzer.

By using this pressure-squared integral, the blast data were also put into a format which could be used to calculate the SEL, which has been shown to be an accurate predictor of community responses.[4]

$$SEL = 10 \log_{10} \int_{-\infty}^{\infty} 10^{L(t)/10} dt \qquad \text{[Eq 3]}$$

where L(t) = the instantaneous weighted sound pressure level in reference to .0002 microbar.

* Blasts were recorded at 1.5 in./sec (3.8 cm/sec) in the field and analyzed at 15 in./sec (38.1 cm/sec). Using the impulse hold response, the 35-msec time constant of the sound level meter appears as 350 msec because of the tenfold increase in the speed of the signal. The resulting level approximates the integral of the squared time-varying signal divided by the constant .035:

$$(\int p^2(t)dt)/.035.$$

Thus, in theory, for a transient whose duration is 350 msec or less, the impulse sound level meter reading should be 4.5 dB above the true integration value for integrations performed with a reference time of 1 sec.

$$\text{Difference} = 10 \log_{10} 1.0/0.35 = 4.5 \text{ dB.}$$

In reality, however, the meter characteristics did not strictly follow this theory. Analysis with tone bursts of varying durations indicated that the sound level meters produce this 4.5-dB difference for transients with durations of 170 msec or less. As the duration increased, the time constant also increased so that for a 350 msec pulse, the constant was 900 msec and the difference between the impulsive reading and true integration was 0.5 dB:

$$\text{Difference} = 10 \log_{10} 1.0/0.9 = 0.5 \text{ dB.}$$

These results explain the shape of the curve in Figure 9. For the higher amplitude peaks occurring at the close-in stations, the duration of tile acoustic signal was less than 170 msec. Thus the difference between the impulse value and $\int p^2(t)dt$ was 4.5 dB. The lower amplitude peaks, occurring at the distant stations, had durations up to and exceeding 350 msec. Thus the difference approached 0 dB and even became negative for greater durations.

4 *Information on Levels of Environmental Noise Requisite to Protect Public Health and Welfare With an Adequate Margin of Safety*, EPA 550/9-74-004 (Environmental Protection Agency, March 1974), p A-6.

Different frequency weightings of the L(t) signal yielded various weighted SEL values, which are discussed in Chapter 7.*

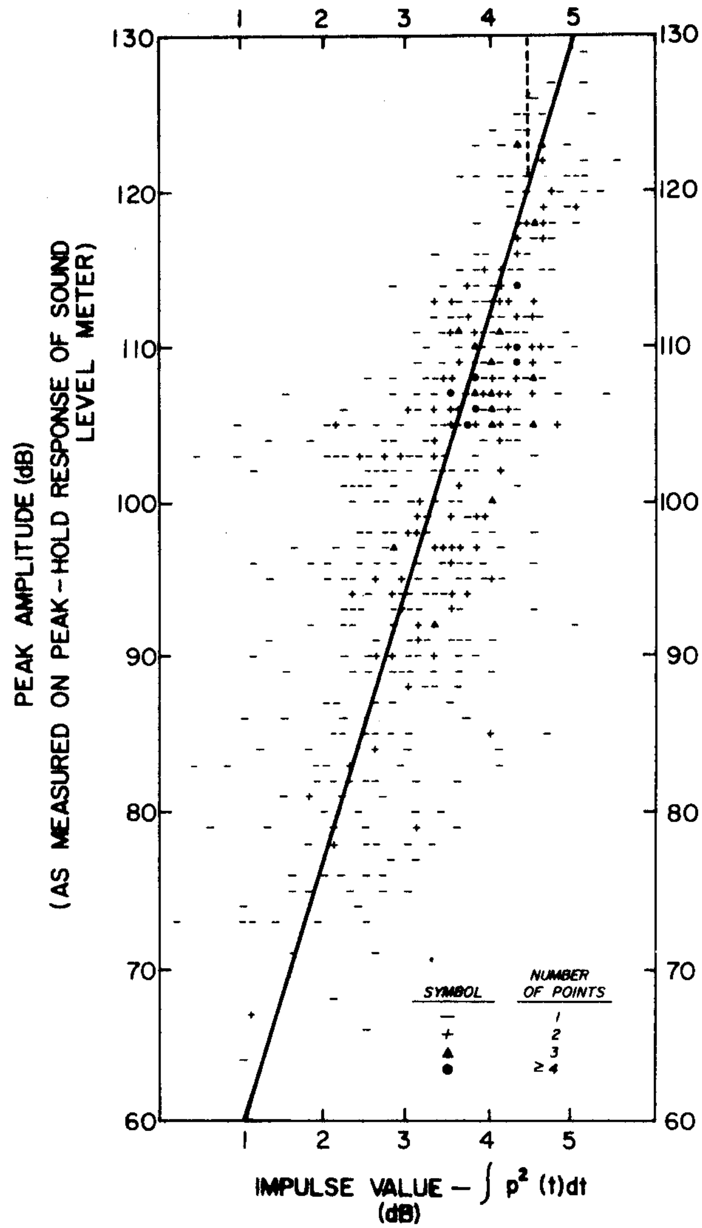

Figure 9. Comparison of pressure-squared integrals, impulse and peak noise levels for different blast signals.

---

* By playing the signal through a sound level meter set on C-weighted slow, a C-weighted SEL was obtained and computed with the Wang calculator. The slow meter characteristics approximate an integrator with a 1-sec reference.

4 Statistics of Blast Propagation

This chapter establishes the statistics of blast propagation in the atmosphere for the acoustic measurements obtained in Chapter 3. The probability of obtaining given amplitudes at various distances is the key statistic. Such probabilities are also required for noise impact prediction. Because these statistics are derived independently of any meteorological or terrain considerations, they form an empirical basis for prediction without explaining why the various levels were recorded.

Before beginning the analysis, the blast data were divided into five categories: (1) good clean blast signatures, (2) data with slight noise present, (3) data containing significant noise but for which there is an accurate measure of the peak value, (4) data for which the peak value could only be estimated, and (5) data missed because of equipment failures or calibration during an event. For statistical analysis of peak values, the first four types of data were both usable and required. Because the lower amplitude events are less likely to be recorded well in the presence of wind and internal equipment noise, excluding category 4 would systematically bias the statistics toward the higher levels.

Using the first three categories of blast data, amplitude distributions were created based on the four distances (2, 5, 10, and 15 mi [3, 8, 16, and 24 km]) and two time periods (0500 to 0700 hours and 0700 to 1100 hours).* Appendix B lists the resulting eight amplitude distributions.

* Noise impact at night (defined as 2200 to 0700 hours by the Environmental Protection Agency) was represented by the 0500 to 0700 hours measurements. The impact during the day (0700 to 2200 hours) was represented by the 0700 to 1100 hours measurements. The 0700 to 0900 hours time period was considered to be a transition from night to day, when the nighttime temperature inversion would normally rise and dissipate. The 0900 to 1100 hours period represented the rest of the day. Since the normal firing at the base was from 0700 to 1500 hours, each measurement taken between 0900 to 1100 hours was used three times to compensate for the fact that this period was also representative of the 1100 to 1300 hours and 1300 to 1500 hours time periods.

As Figures 10 and 11 show, each individual distribution could be subdivided into four ranges using three natural breaks. After minor variations in these initial breakpoints (1 to 2 dB) were made to create more uniform distribution curves, the energy averages of the measured blasts within each range were calculated. These levels were plotted as a function of distance to produce the amplitude distance curves in Figure 12.

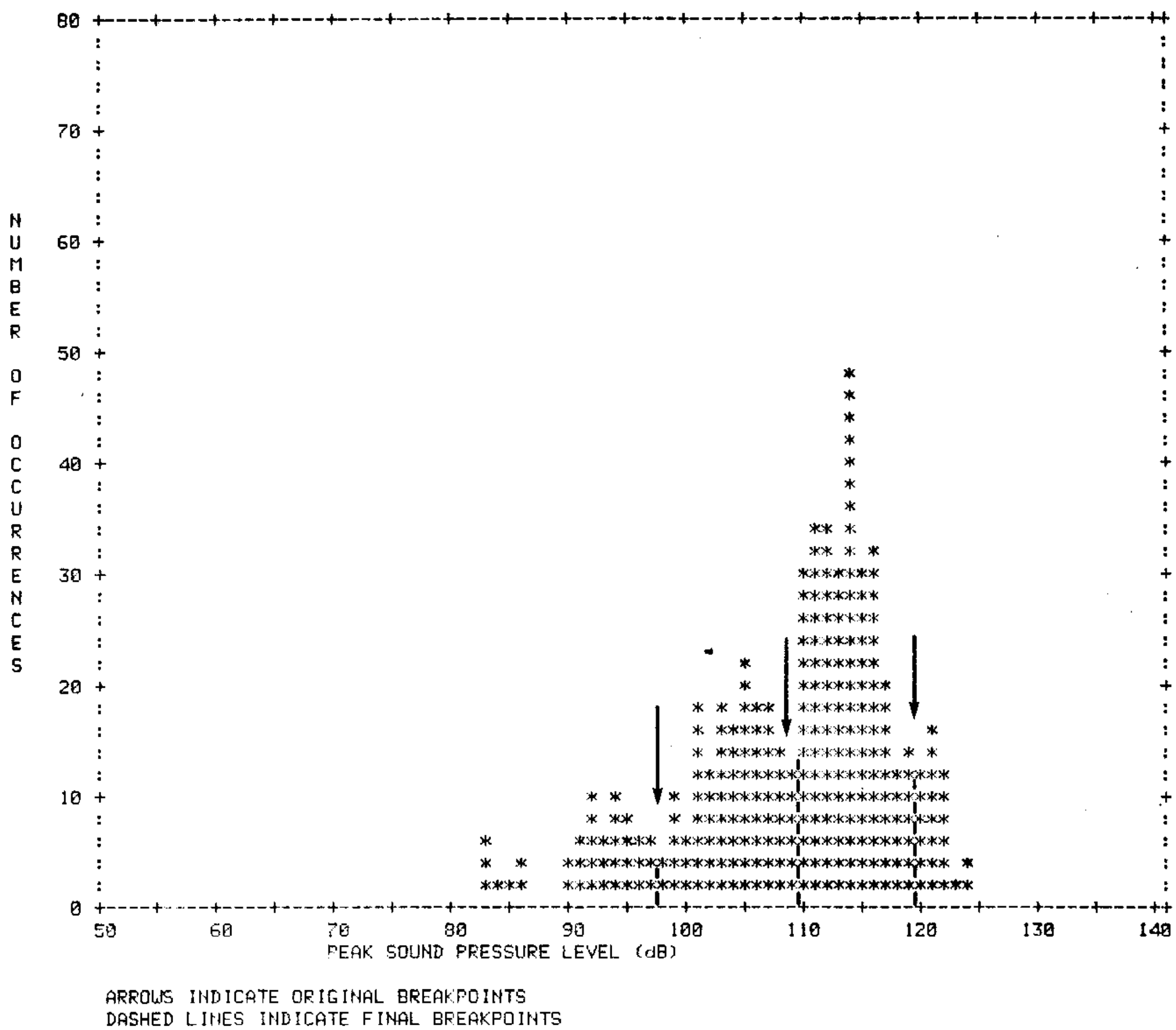

Figure 10. Two-mi nighttime peak sound pressure level distribution (original and final breakpoints).

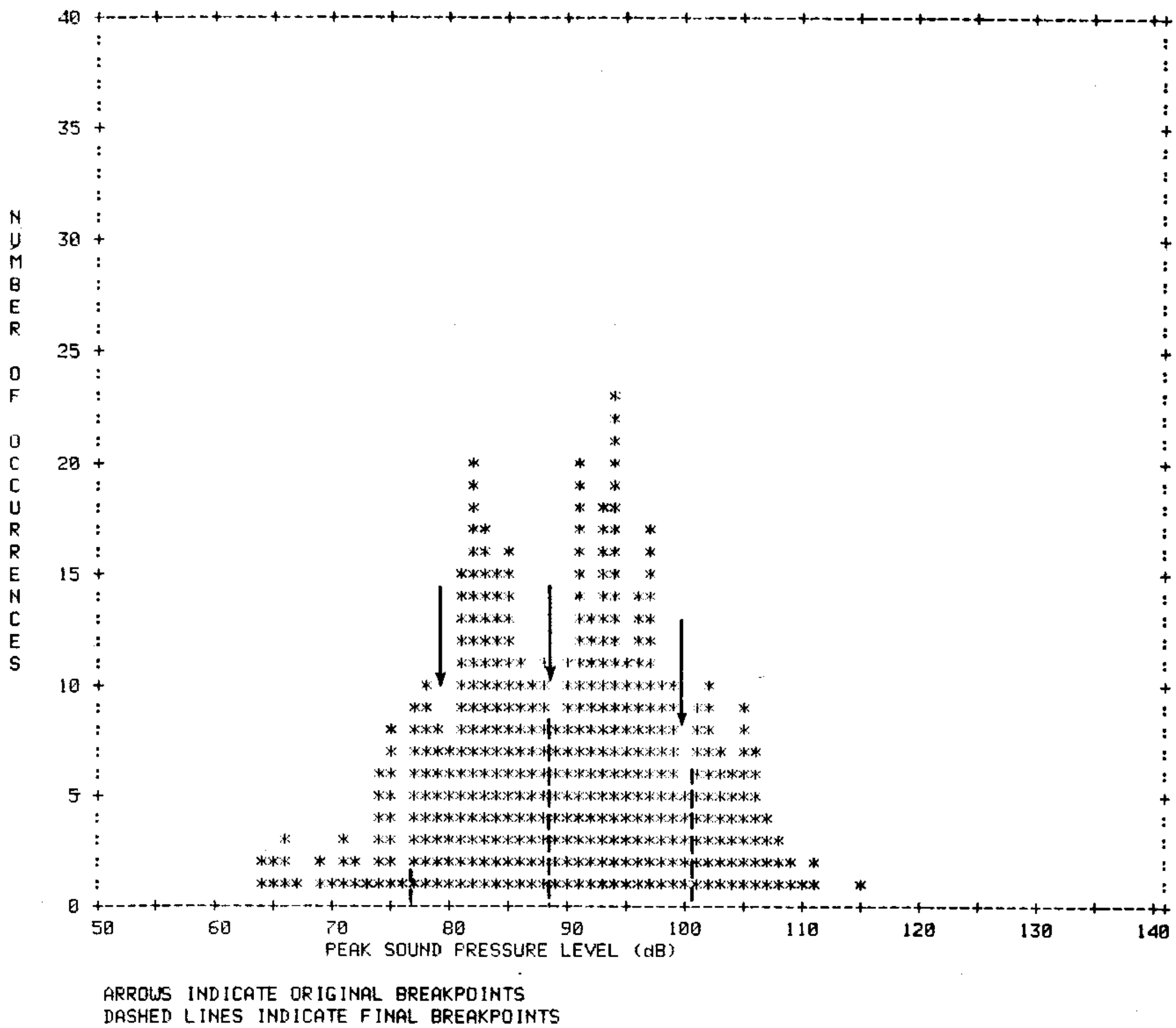

Figure 11. Ten-mi nighttime peak sound pressure level distribution (original and final breakpoints).

The low amplitude blast data in category 4 were then added to the appropriate distributions so that the percentage of blasts lying in each range could be determined for each distribution. These calculations are summarized in Table 2 and detailed in Appendix B. While Table 2 relates percentage of amplitudes to distance, it does not explain the high or low levels. Before an explanation could be developed, the statistics had to be related to weather and terrain, as detailed in Chapter 5.

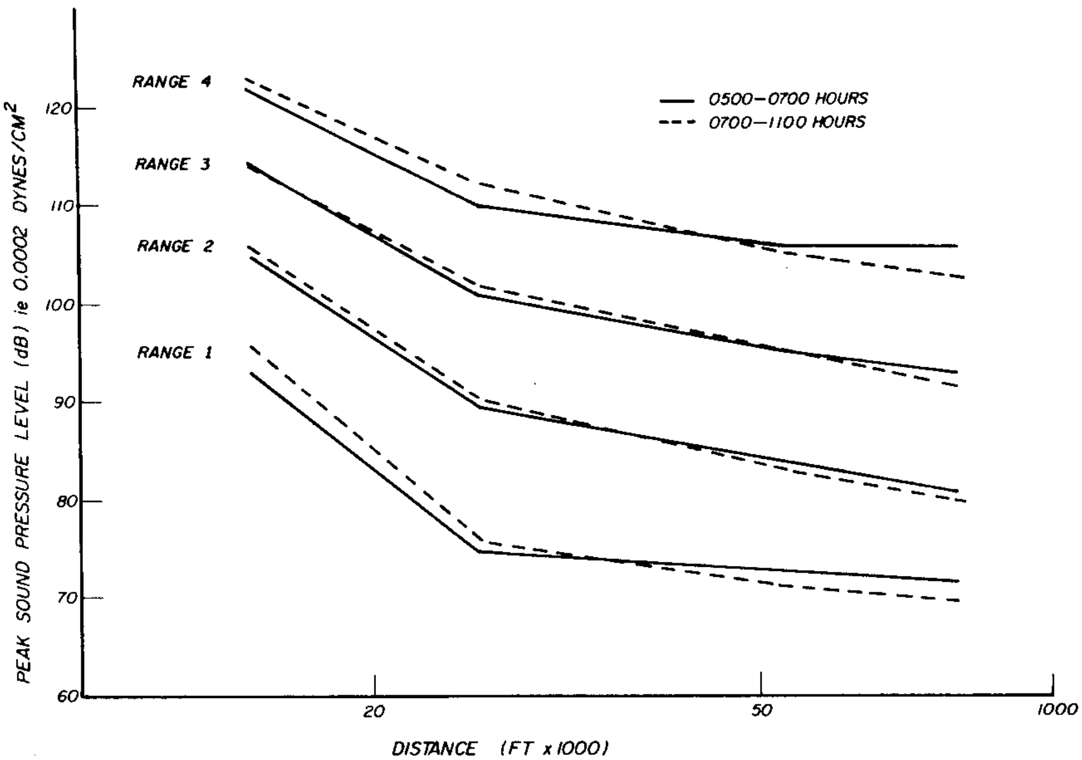

Figure 12. Measured amplitude versus distance curves.

Table 2. Statistics of blast propagation for the eight amplitude distributions.*

	Distance			**Range**	
Time	**mi (km)**	**1**	**2**	**3**	**4**
0500 to	2 (3.2)	93.0 dB	105.1 dB	114.6 dB	121.9 dB
0700 hours		25.4%	29.5%	39.0%	6.1%
	5 (8.0)	74.8 dB	89.3 dB	101.0 dB	110.0 dB
		18.4%	24.8%	49.2%	7.6%
	10 (16.1)	72.8 dB	83.8 dB	95.1 dB	105.8 dB
		47.9%	25.0%	20.0%	7.1%
	15 (24.1)	71.6 dB	80.5 dB	92.7 dB	105.3 dB
		45.2%	33.7%	16.7%	4.4%
0700 to	2 (3.2)	95.7 dB	105.9 dB	114.3 dB	123.0 dB
1100 hours		37.5%	39.6%	20.6%	2.3%
	5 (8.0)	75.9 dB	90.0 dB	102.0 dB	112.2 dB
		37.5%	39.6%	20.6%	2.3%
	10 (16.1)	71.1 dB	83.1 dB	95.0 dB	105.3 dB
		25.9%	32.6%	31.8%	9.7%
	15 (24.1)	69.1 dB	79.9 dB	91.6 dB	102.3 dB
		34.8%	32.1%	30.0%	3.1%

*Categories 1 through 4 were used to determine percentages; categories 1 through 3 were used to determine energy averages.

5 Comparison of Blast Propagation Statistics with Theoretical Amplitude/ Distance Prediction Curves

In this chapter, the blast propagation statistics developed in Chapter 4 — specifically, the amplitude versus distance plot — are compared to the theoretical prediction curves in CERL Technical Report E-17.[5] Because these curves were based on meteorological conditions, this comparison can indicate a weather dependence.

The curves in CERL Technical Report E-17 are based on theory for sound propagation in the atmosphere. This theory is discussed in many references,[6] which show that speed of sound is a function of both wind and temperature, and as these conditions change with altitude, sound waves are refracted or focused. Figures 13 through 16 illustrate four simple cases of this phenomenon: (1) a negative sound velocity gradient, (2) a positive sound velocity gradient, (3) a positive sound velocity gradient which changes to a more sharply positive velocity gradient, and (4) a negative gradient followed by a positive gradient at a higher altitude.

In Case 1, the sound is refracted upward, producing noise levels on the ground lower than those produced under uniform velocity or zero gradient conditions. For Case 2, sound rays are refracted down, and the sound intensity on the ground is somewhat greater than that under uniform velocity gradient conditions. With combinations of these gradients, the sound rays can travel over different paths and still arrive at an observation point simultaneously to produce a focus. In Case 3, separate groups of sound rays are created by two positive gra-

[5] P. D. Schomer, *Predicting Community Response to Blast Noise,* Technical Report E-17/AD773690 (CERL, 1973) pp 13, 17.

[6] B. Perkins, Jr., P. H, Lorrain, and W. H. Townsand, *Forecasting the Focus of Air Blast Due to Meteorological Conditions in the Lower Atmosphere,* Report No. 1118 (Ballistics Research Laboratories, 1960); J. W. Reed, *Acoustic Wave Effects Project: Air-blast Prediction Techniques,* Report SC-M-69-332 (Sandia Laboratories, 1969); and Schomer.

dients — the upper gradient stronger than the lower. A weak focus, labeled f, is created at the points where both groups meet at the surface. In Case 4, sound is refracted upward in the lower negative gradient and downward in the upper positive gradient. The result is an increase of noise levels at the sharp focus in the region labeled F and a reduction of noise levels in the silent zone between F and the blast site.

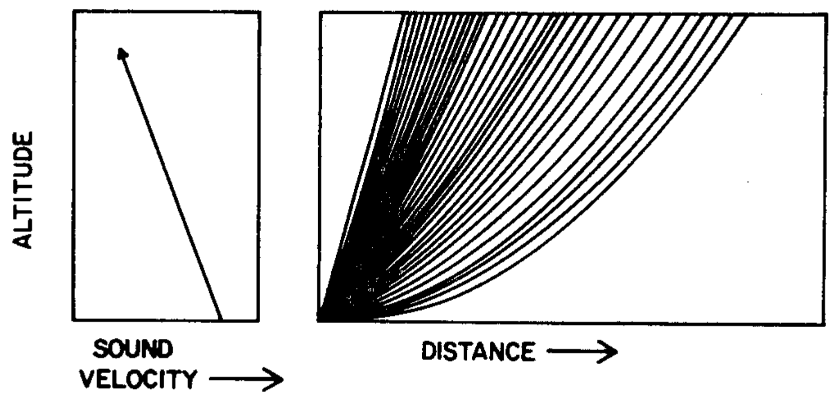

Figure 13. Negative sound velocity gradient and corresponding ray paths.

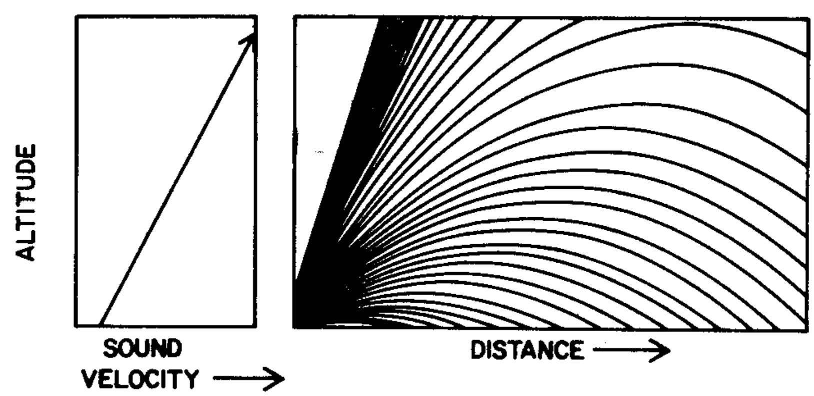

Figure 14. Positive sound velocity gradient and corresponding ray paths.

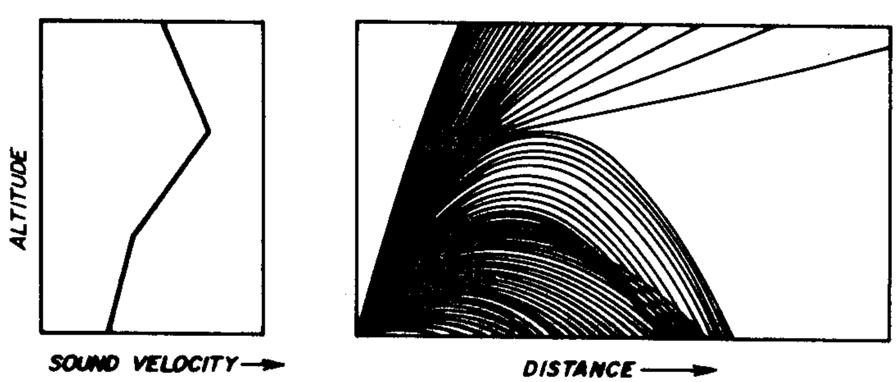

Figure 15. Two-segmented positive sound velocity gradient and corresponding ray paths (weak focus is located at f).

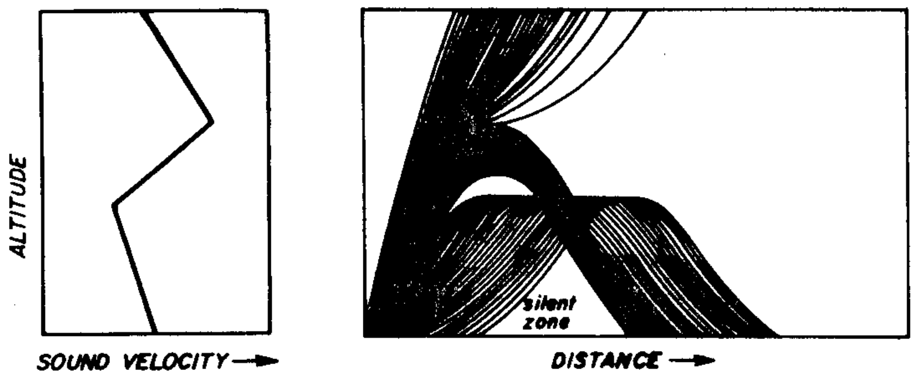

Figure 16. Negative-positive sound velocity gradient (inversion) and corresponding ray paths (strong focus is located at F).

Using this information, CERL Technical Report E-17 created a set of prediction curves to estimate the peak blast amplitude on the basis of distance and meteorological conditions; Figure 17 shows these prediction curves.* The curve labeled "base" is the IBM M-curve for ideal atmospheric or zero gradient conditions compiled in Sandia Laboratories Report SLM-69-332.[7] Blast amplitudes recorded during positive gradients should be a little higher than this curve, while blasts recorded in negative gradients estimated by the negative gradient curve, should be lower. The probable focus and maximum overpressure curves estimate the probable and maximum peak amplitudes, respectively, under focus conditions.

To compare the blast propagation statistics and these curves, the amplitude distance plots from Chapter 4 were directly transposed onto Figure 17 (Figures 18 and 19).

* The curves in Figure 17 were derived for 1-lb (0.5 kg) charges exploded just above ground level. Energy loss due to absorption was avoided, but sound was reflected. At Fort Leonard Wood, the charges weighed 5 lb (2.3 kg) and were exploded at ground level with both absorption and reflection occurring. Therefore, the following two correction factors were applied to the prediction curves: 5.6 dB was added to adjust for the extra weight and 5.5 dB was subtracted to adjust for the difference between above-ground and ground-level blasts. The 5.5 dB subtraction is based on the fact that the blast site was soft, dry, pulverized ground which was expected to absorb a great amount of energy. The two correction factors almost cancelled each other out.

[7] J. W. Reed, *Acoustic Wave Effects Project: Airblast Prediction Techniques*, Report SC-M-69-332 (Sandia Laboratories, 1969).

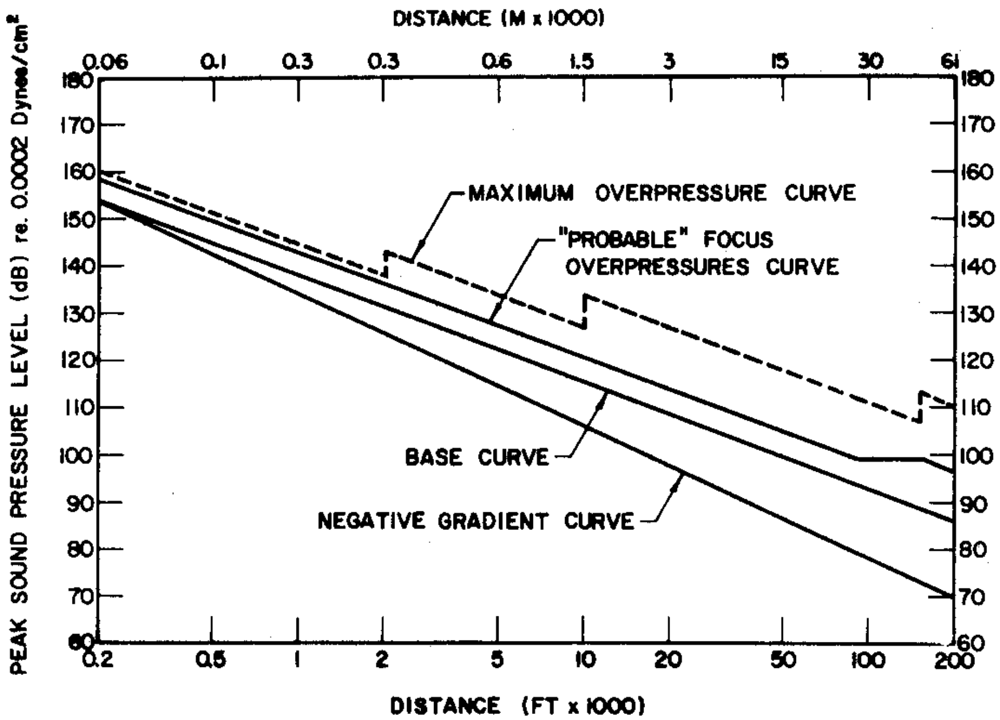

Figure 17. Theoretical amplitude versus distance prediction curves from CERL Technical Report E-17.

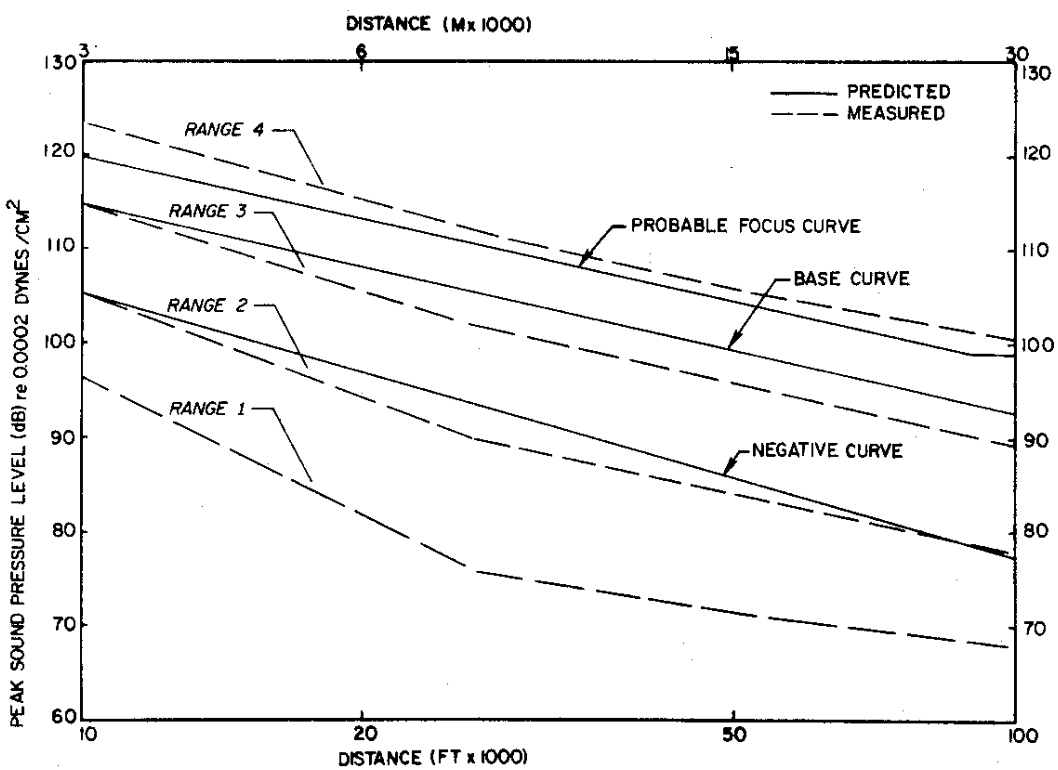

Figure 18. Comparison of measured peak amplitudes (day) to prediction curves.

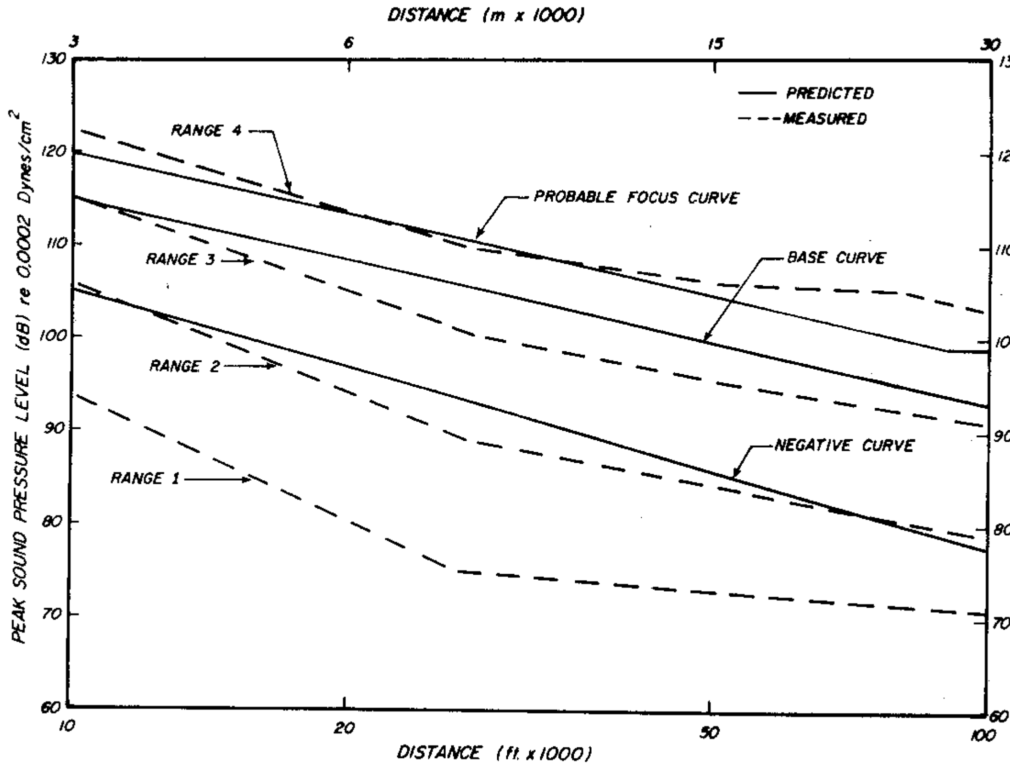

Figure 19. Comparison of measured peak amplitudes (night) to prediction curves.

The data from range 4 generally plotted above the probable focus curve due to the conservative original estimates in CERL Technical Report E-17. The range 3 data dropped a few decibels beneath the base or IBM curve; this drop probably resulted from the relatively low blast amplitudes employed in the test in contrast to the large amplitudes obtained in previous tests, such as those resulting from nuclear devices. Data from range 2 agreed quite closely with the negative curve, while range 1, which fell below all the prediction curves, was put into an “excess negative” designation. This close agreement between plots implies a relationship between the energy amplitudes in ranges 2 through 4 and specific weather conditions (Table 3).

The data in range 4 indicate that a new focus curve can be plotted and used to predict amplitudes under focus conditions. Similarly, new base and negative curves can possibly be plotted from the data in ranges 3 and 2, respectively, and used to predict amplitudes under those specific weather conditions. The data in range 1 created the unique excess negative curve which fell below all the curves in CERL Technical Report E-17.

Table 3. Relationship between energy amplitudes and weather conditions.

Range	Curve	Weather Condition
1	Excess Negative	–
2	Negative	Shadow and Gradient
3	Base	Zero and Positive Gradient
4	Focus	Focus

Finally, Figure 20 compares the actual maximum reading obtained at each distance to the maximum probable focus curve. Since these data were based on approximately 11,000 samples, they offered good verification of the curve, which can be used to protect against structural damage and other extreme effects.

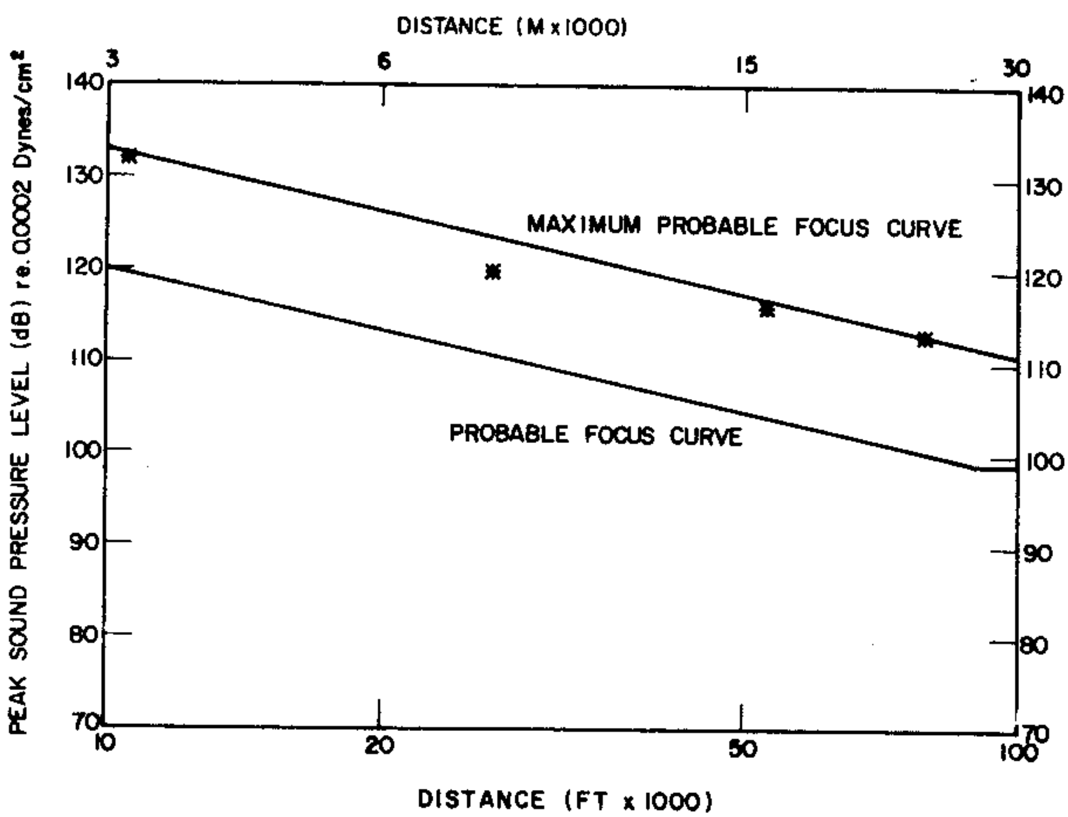

Figure 20. Predicted and measured maximum probable focus.

6 The Effect of Terrain and Meteorological Conditions on Blast Propagation

The analysis in Chapter 5 implied a possible relationship between blast amplitudes and meteorological conditions for the Fort Leonard Wood data. This chapter confirms the relationship by analyzing individual blasts with the amplitude versus distance curves developed in Chapter 4. The effects of terrain are also discussed.

Effect of Meteorological Conditions

Although an ideal study of individual blast propagation would require knowledge of meteorological conditions at all points within the space of interest at the time of propagation, obtaining such extensive information was impractical. Because the FAA plane takes substantial time to climb from ground level to the upper altitude, the data obtained was a function of altitude only at one area. Thus it was assumed that this gradient does not change laterally with distance. Since inversion heights, winds, and other factors change as a function of position over the ground, this assumption could yield misleading results and was thus used cautiously. In addition, the analysis of individual blasts had to be based on a much smaller number of gradients than desired.

A total of 735 blasts were measured at Fort Leonard Wood. Ten to twelve blasts occurred each hour, 5 to 6 minutes apart. The FAA plane gathered temperature data three or four times each hour, while upper altitude wind information was gathered a maximum of three times per day. The time available for data-gathering was limited by pre- and postflight calibrations as well as the time required to reach the outer 15 mi (24 km) stations and prepare for the run.

Based on these considerations, the measured blast data and the meteorological conditions were correlated as follows. Temperature information, recorded three or four times each hour, was placed into two categories: (1) information from temperature runs made either directly before or after a wind run, and (2) information from temperature runs made both before and after other temperature runs (Table 4).

Table 4. Sample log of temperature and wind runs.

Day	Start Time	Finish Time	Run	Category
06/13	0837	0842	Temp	2
	0850	0855	Temp	2
	0906	0910	Temp	2
	0918	0922	Temp	1
	0923	0930	Wind	–
	0936	0941	Temp	1
	0954	0957	Temp	2
	1000	1005	Temp	1
	1005	1010	Wind	–
	1017	1022	Temp	1

The temperature runs in category 1 were combined with the closest (in time) wind run to produce sound velocity profiles in the north, east, south, and west directions based on the procedures in Chapter 3. Next, using the methods in Ballistic Research Laboratories (BRL) report 1118,[8] conditions favorable to the different focusing or refracting modes of sound waves were established. Figure 12 was used to predict the amplitudes for each condition: the focus curve was used for focus conditions, the base curve for positive gradient conditions, and the negative curve for negative gradient conditions and shadow zones. Finally, the measured amplitudes for blasts occurring when this weather information was taken were compared to these predicted levels.

As an example, in Table 4 the temperature run from 0918 to 0922 was combined with the wind run from 0923 to 0930 to produce sound velocity gradients, which were used to predict the amplitudes for blasts occurring between 0918 and 0930. The temperature run from 0936 to 0941 was then combined with the wind run from 0923 to 0930, and the process was repeated. Blast amplitudes falling outside these critical time periods were not used in this analysis, because the weather data would not be current enough to give reliable results.*

[8] B. Perkins, Jr., P.H. Lorrain, and W.H. Townsand, *Forecasting the Focus of Air Blast Due to Meteorological Conditions in the Lower Atmosphere,* Report 1118 (Ballistics Research Laboratories, 1960).

* In addition to this temporal constraint, only tape-recorded data from the following three categories of blast signatures were used in this analysis: (1) good, clean blast signatures; (2) data with slight noise present; and (3) data containing significant noise but for which there was an accurate measure of the peak value. Out of the 11,760 total measurements (735 blasts x 16 sites), 1841 measurements occurring in the critical time periods met these criteria.

Approximately 66.0 percent of the 1841 usable blast measurements fell within 7 dB of the predicted values; Figure 21 shows three examples of this agreement. The data which disagreed could be divided into the following categories:

1. Excess Shadow (ES) - lower than predicted levels measured during shadow zone conditions
2. Excess Negative (EN) - lower than predicted levels measured during negative gradient conditions
3. Excess Positive (EP) - lower than predicted levels measured during positive gradient conditions
4. Missed Focus (MF) - lower than predicted levels measured during focus conditions
5. Missed Shadow (MS) - higher than predicted levels measured during shadow conditions
6. High Negative (HN) - higher than predicted levels measured during negative gradient conditions
7. High Positive (HP) - higher than predicted levels measured during positive gradient conditions
8. High Focus (HF) - higher than predicted levels measured during focus condition.

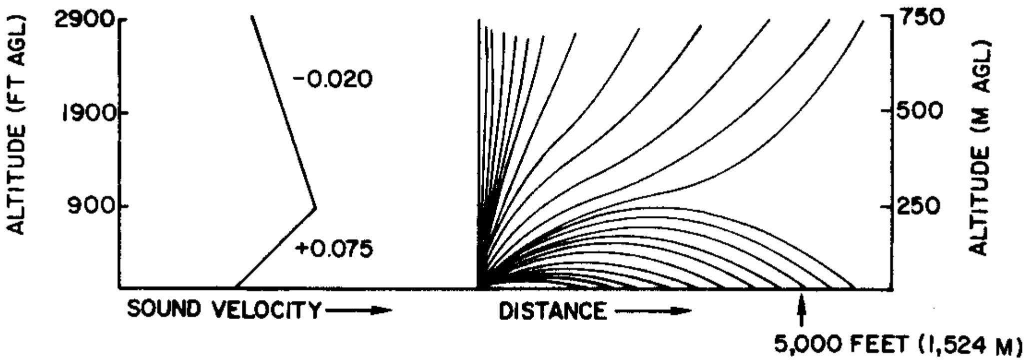

Positive gradient prediction at 2-mi station
Predicted peak sound pressure level 115 dB
Measured peak sound pressure level 118 dB

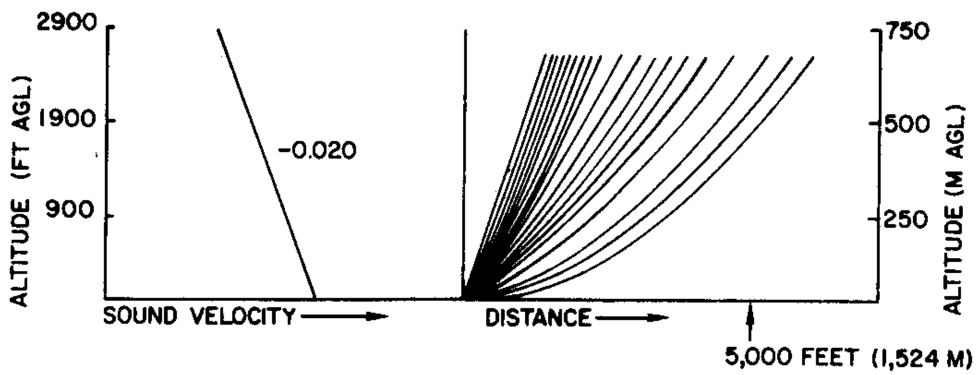

Negative gradient prediction at 2-mi station
Predicted peak sound pressure level 106 dB
Measured peak sound pressure level 108 dB

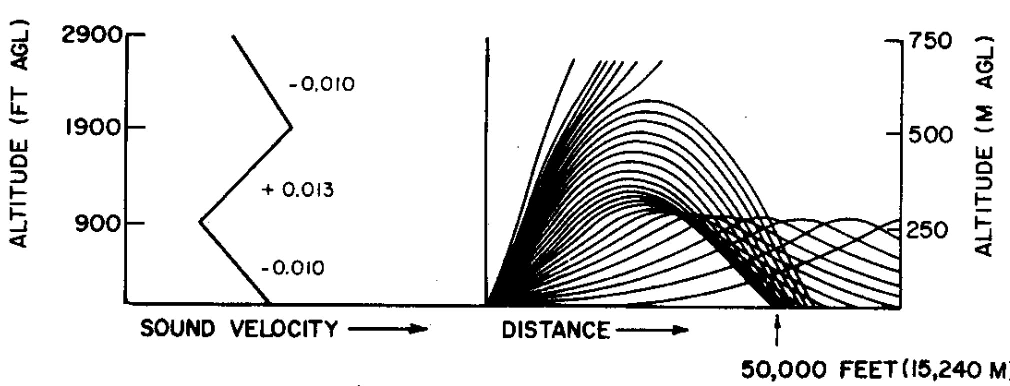

Focus prediction at 10-mi station
Predicted peak sound pressure level 105 dB
Measured peak sound pressure level 103 dB

Figure 21. Prediction of peak amplitudes during focus, positive gradient, and negative gradient conditions.

Table 5 summarizes the initial comparison analysis.

Of the disagreement data, the number of measurements falling below the predicted levels far exceeded the number falling above. In an attempt to correlate these data, the meteorological listings in Appendix A were re-examined to summarize the general weather conditions experienced when these measurements were taken. Table 6 shows the results, which were used to resummarize the disagreement data (Table 7).

Table 5. Summary of initial comparison analysis.

	Number	Disagreement								
Prediction	**Agreement**	**ES**	**MS**	**EN**	**HN**	**EP**	**HP**	**MF**	**HF**	**Total**
Shadow	407	80	76							156
Negative	241			167	45					212
Positive	437					119	28			147
Focus	129							111	1	112
Total	1214									627

Table 6. General weather conditions present during disagreement measurements.

Type of Disagreement	Weather Conditions
Excess Shadow Excess Negative	Upwind or crosswind station, strong negative gradient (<-.030 m/sec/m)
Excess Positive	Upwind station, weak positive gradient (<.005 m/sec/m) Downwind station, sharp positive gradient (>.075 m/sec/m)
Missed Focus Missed Shadow	Not weather-related; caused by inability to exactly predict focus/shadow position
High Negative	Wind reversal or wind shear
High Positive	Weak focus conditions
High Focus	–

Table 7. Summary of disagreement data.

Type of	Total	Condition		
Disagreement	**Number**	**1**	**2**	**Unexplained**
Excess Shadow	80	35	–	45
Excess Negative	167	117	–	50
Excess Positive	119	25	77	17
Missed Focus	111	111	–	–
Missed Shadow	76	76	–	–
High Negative	45	20	–	25
High Positive	28	25	–	3
High Focus	1			1
Total	627	409	77	141

The first column of Table 7 lists the type of disagreement, while the second lists the total number of disagreement measurements. The next two columns list the number of disagreement measurements obtained under the conditions listed in Table 6. The following paragraphs present a more detailed analysis:

1. Excess Shadow. Eighty measurements taken during shadow conditions were lower than the predicted levels. Of these, 35 were taken at stations located upwind, under a strong negative gradient (less than -.030 in./sec/in. [-.030 m/sec/m]). While these conditions do not physically explain the low result, they do correlate them with a particular set of conditions. The remaining 45 measurements could not be physically explained or correlated with any set of conditions.

2. Excess Negative. A total of 167 measurements taken during negative gradient conditions were lower than the predicted levels. Of these, 117 were taken at stations located upwind, under a strong negative gradient (less than -.030 in./sec/in. [.030 m/sec/m]). While these conditions do not physically explain the results, they do correlate them with a particular set of conditions. The remaining 50 measurements could not be physically explained or correlated with any set of conditions.

3. Excess Positive. A total of 119 measurements taken during positive gradient conditions were lower than the predicted levels. Of these, 25 were taken at stations located upwind, under a weak positive gradient (less than .005 in./sec/in. [.005 m/sec/m]). Under these conditions, it is possible that wind gusts could shift the weak positive gradient to a negative one, thus accounting for the low amplitudes. This condition represents a possible physical explanation of the disagreement measurement.

Of the remaining excess positive data, 77 readings were taken at stations located downwind, under a strong positive gradient (greater than .075 in./sec/in. [.075 m/sec/m]). This observation is merely a correlation with a particular set of conditions. The remaining 17 measurements could not be physically explained or correlated with any set of conditions.

4. Missed Focus/Missed Shadow. A total of 111 measurements taken during focus conditions were lower than predicted, while 76 measurements taken during shadow conditions were higher than predicted. The missed focuses occurred because the exact time and location of a focus could not be pinpointed with the existing weather data. In other words, the focus was near but not at the specific location at the time in question; it appeared either shortly before or after the predicted time. Table 8 is an example of this situation. Although a 5-mi (8 km)

focus was predicted at 0824 hours, the recorded levels indicated that focuses occurred at 0836 and 0842 hours instead. Since focuses are rather "sharp," the rest of the readings were measured in a shadow zone. All of the 111 Missed Focus readings could be related to this inability to predict the exact focus position.

Table 8. Time dependence of a focus.

Blast Number	Time	Peak Sound Pressure Level (dB)
709	0800	106
710	0812	106
711	0816	106
712	0820	105
713	0824	110*
714	0830	111
715	0836	114**
716	0842	113**
717	0848	104
718	0854	99

* Prediction of focus

** Occurrence of focus.

Station: East 5 mi. (8.0 km)

Similarly, all of the 76 missed shadow readings could be attributed to the same problem occurring when focus observations were made in a predicted shadow zone. Since focuses are sharp and shadow zones broad, it was expected that the number of missed focuses would greatly exceed the number of missed shadows. These conditions represent physical explanations for all the disagreement measurements in these categories.

5. High Negative. A total of 56 measurements taken under negative gradient conditions were higher than the predicted levels. Of these, 20 readings were made under wind shear conditions, where there was a wind reversal of at least 90 degrees at a higher altitude. These measurements were made at both upwind and downwind stations. While the wind shear condition does not physically explain the high results, it does correlate them with a set of conditions. The remaining 25 readings could not be physically explained or correlated with any set of conditions.

6. High Positive. A total of 28 measurements taken during positive gradient conditions were higher than the predicted levels. Of these, 25 were made under the weak focus condition described in Chapter 5, which represents a possible physical explanation of the disagreement measurements. The remaining three high positive readings could not be physically explained or correlated with any set of conditions.

7. High Focus. Because only one measurement was higher than predicted during focus conditions, no attempt was made to correlate the amplitudes with meteorological data. One hypothesis, however, is that this result was caused by a very sharp focus.

In the previous paragraphs, the disagreement data were placed into the following three groupings:

1. Data which could be physically explained
2. Data which could be correlated with a specific set of meteorological conditions
3. Data which could not be explained or correlated with any set of conditions.

Both the physical explanations and correlations indicated conditions which produced measured amplitudes either higher or lower than the predicted levels. For example, wind shears tended to produce higher-than-predicted negative amplitudes, while a strong negative gradient tended to produce lower-than-predicted negative amplitudes. However, it should be noted that these conditions represented trends rather than absolute rules; in many cases, measurements made in wind shears were lower than the predictions, while those made in strong gradients were higher. Table 9 summarizes the measurements made under each of the weather conditions listed in Table 6.

Table 9 is divided into three major columns. The first summarizes measurements made under conditions correlated with higher-than-predicted amplitudes. While some measurements were lower than predicted and others in agreement, a vast majority followed the trend toward higher-than-predicted levels. For example, 44 measurements were made during a negative gradient and a wind shear; of these, 20 were higher than predicted, 21 were in agreement, and three were lower than predicted. A similar analysis is shown for amplitudes obtained in conditions correlated with missed shadows and high positives. The third column summarizes measurements made in conditions correlated with lower-than-predicted amplitudes. While some were higher than predicted and others in agreement, a significant majority followed the trend toward lower-than-predicted levels. The middle column summarizes the measurements made under conditions which are not correlated to disagreement data in Table 6. As expected, a significant majority of the measurements agree with the predicted results. These results show that the physical explanations and correlations listed in Table 6 did not produce reliable trends for the disagreement data.

Table 9. Summary of physical explanations/correlations.

	Column 1 Measurements Made Under Conditions Correlated with Higher-Than-Predicted Levels				Column 2 Measurements Made Under None of the Conditions Listed in Table 6			Column 3 Measurements Made Under Conditions Correlated with Lower-Than-Predicted Levels			
Prediction	Condition	Number Higher Than Predicted	Number Agreeing with Prediction	Number Lower Than Predicted	Number Higher Than Predicted	Number Agreeing with Prediction	Number Lower Than Predicted	Condition	Number Higher Than Predicted	Number Agreeing with Prediction	Number Lower Than Predicted
Shadow	MS	76	--	--	--	327	45	ES*	11	80	35
Focus	HF	--	--	--	1	129	--	MF	--	--	111
Negative	HN	20	21	3	25	223	50	EN	9	36	117
Positive	HP	25	17	8	3	335	17	EP**	6	155	92
Total***	--	121	38	11	29	1014	112	--	26	271	355

* It should be noted that there were significantly more agreement measurements in this section than low readings. However, the percentage of low readings (35 out of 126) is still significantly higher than the percentage of low readings (45 out of 327) in the second column.

** It should be noted that there were significantly more agreement readings in this section than low readings. However, the percentage of low readings (92 out of 253) is still significantly higher than the percentage of low readings (17 out of 355) in the second column.

*** Total number in this table will exceed the actual 1841 measure blasts because of overlapping conditions. For example, conditions producing HN and EN readings occurred simultaneously on certain occasions, as did conditions producing EP and HP results.

Table 10 summarizes the entire prediction analysis.

Table 10. Summary of final prediction analysis.

Prediction	Number of Agreements	Type of Disagreement	Total	Number Physically Explained	Number of Disagreements Correlated	Unexplained
Shadow	407	ES	80		35	45
		MS	76	76		
Negative	241	EN	167		117	50
		HN	45		20	25
Positive	437	EP	119	77	25	17
		HP	28	25		3
Focus	129	MF	111	111		0
		HF	1			1
Total	1214		627	289	197	141
	(66.0%)		(34.0%)	(15.7%)	(10.7%)	(7.6%)

Effect of Terrain

Although the percentages in Table 10 indicate that blast amplitudes have a high degree of dependence on weather conditions, it appears that these results would improve significantly if barrier effects were considered. At the 2- and 5-mi (3 and 8 km) stations in both the south and west directions, terrain effects prevented a direct line of sight to the blast area. Since these barriers would produce lower levels than predicted, they might account for the previously unexplained disagreement data. To verify this hypothesis, the amplitude data were analyzed without the measurements made at these four stations (Table 11).

Table 11. Barrier effects.

	Number (Percentage)			
Category	**All Data**		**Partial Data**	
Agreement	1214	(66.0)	934	(70.5)
Physically Explained	289	(15.7)	257	(19.4)
Correlated	197	(10.7)	62	(04.7)
Unexplained	141	(07.6)	71	(05.4)
Total	1841	(100.0)	1324	(100.0)

As expected, the percentage of agreement data and physically explained data increased, while the percentage of unexplained data decreased, indicating that the barriers did have a significant effect on these areas. However, the decreasing percentage of correlated data was an unexpected result.

Nonetheless, the high degree of correlation between measured amplitudes (with or without the barrier effect) and predicted levels provides further evidence of a weather dependence, and more significantly, indicates that the prediction curves defined in Figure 12 gave reliable results.

Effect of Distance, Wind Direction, and Time of Day

Figure 22 illustrates an additional relationship between surface wind direction, time of day, and distance.* In this figure, the data are divided into 144 cells based on the following categories:

1. Four basic sound velocity profile categories (double negative, double positive, positive-negative, and negative-positive gradient)
2. Three time periods (0500 to 0700 hours, 0700 to 0900 hours, and 0900 to 1100 hours)
3. Four distances (2, 5, 10, and 15 mi [3, 8, 16, and 24 km])

---

* Blast data from categories 1 through 4, as explained on page 24, were considered for this analysis. However, since only directions within ± 30 degrees of crosswind, downwind, or upwind were used to increase the chance of finding a significant relationship, the actual number of measurements was limited to 6739.

4. Three wind directions (downwind, crosswind, and upwind).

The number of blast measurements and the energy average level were entered in each cell; the cells were than aggregated into 16 larger groups based on the four sound velocity profiles and the four distances. Within each group, the three time periods were examined; if one was significantly larger than the others, it was marked with a square for downwind locations and a circle for upwind locations. (No crosswind locations were found to have the highest level.)

This analysis revealed that at the shorter distances and at later hours in the day the downwind stations recorded the highest amplitude levels. At greater distances and at earlier hours of the day, the upwind stations recorded the highest amplitude levels. This was a rather unexpected result, since it is contrary to results given in the literature; however, earlier studies did not measure noise in the early morning hours. The fact that downwind stations do not always experience the highest noise levels is quite significant in predicting both noise levels and community response.

DISTANCE

TIMES
1=0500-0700
2=0701-0900
3=0901-1130

CATEGORY	TIME	2 mi (1.6 km) Wind Direction From			5 mi (8.0 km) Wind Direction From			10 mi (16.1 km) Wind Direction From			15 mi (24.1 km) Wind Direction From		
		From	Cross	Toward	From	Cross	Toward	From	Cross	Toward	From	Cross	Toward
NN	1	109.8 4	109.4 51	110.0 24	92.5 8	97.0 47	102.7 29	0	82.7 19	103.9 31	0	92.5 17	80.8 9
NN	2	109.7 35	103.0 82	95.1 14	98.9 36	88.3 71	81.7 3	94.0 28	90.6 40	80.7 3	73.1 7	89.8 15	0
NN	3	108.6 24	103.8 85	94.0 49	95.6 25	87.5 84	73.4 19	88.4 16	95.6 32	92.0 1	80.0 2	86.7 23	0
PP	1	108.7 69	106.4 98	92.9 18	92.7 67	93.4 129	106.0 39	92.0 13	85.8 52	95.8 39	83.7 3	90.0 26	80.5 2
PP	2	111.8 70	106.9 115	93.8 28	100.2 65	100.1 99	91.1 59	87.9 30	91.5 78	98.9 47	83.9 17	91.3 72	89.4 15
PP	3	110.9 53	101.4 68	95.5 29	101.9 46	90.2 43	83.1 23	91.5 33	91.5 59	101.0 6	87.8 20	87.0 26	90.8 4
PN	1	111.9 45	117.1 41	117.0 2	100.1 71	88.5 71	98.5 22	77.7 26	81.4 27	86.6 24	79.5 22	0	88.9 14
PN	2	113.4 7	110.4 43	101.5 2	98.4 26	100.8 43	82.5 6	87.8 4	97.4 39	95.0 4	70.6 5	92.7 29	87.5 2
PN	3	107.2 47	107.4 55	96.8 13	102.7 35	90.7 44	77.6 18	92.1 32	87.6 23	83.2 13	87.4 14	87.0 12	0
NP	1	0	105.2 12	99.8 28	0	103.8 1	95.3 25	0	89.9 11	98.2 33	0	85.0 1	93.8 30
NP	2	107.3 6	102.3 23	92.6 27	109.5 6	96.3 19	87.4 19	92.9 7	92.2 12	95.9 10	80.0 2	91.5 6	98.9 11
NP	3	107.6 7	100.3 46	87.4 5	103.3 6	87.2 24	72.4 9	93.7 6	89.1 37	93.2 5	82.0 1	85.4 11	87.0 1

Figure 22. Peak sound pressure level dependence on surface wind direction, time of day, and distance.

7 Spectral Content of Blast Noise

Appendix C (Volume II) lists the one-third octave spectra calculated for most blast recordings in Chapter 3.* From those data, energy average and normalized energy average one-third octave spectra were derived for various groupings (time, meteorological condition, distance, direction, etc.). In addition, such physical descriptors as the flat-, C-, and A-weighted SEL were obtained for these groupings and for individual blasts. This chapter details these calculations and determines meteorological effects on spectra.

First, the blast data were divided into 75 categories based on five weather conditions (excess negative, negative, base, focus, and all), five distances (2, 5, 10, and 15 mi [3.2, 8, 16, and 24 km] and all), and three time periods (0500 to 0700 hours, 0700 to 1100 hours, and all). For each category, the energy average one-third octave spectrum (X) was computed for each frequency band using Eq 4.

$$X = 10 \log_{10} \frac{1}{n} \sum_{i=1}^{n} 10^{L_i/10} \qquad \text{[Eq 4]}$$

Where n = number of blast measurements in a given category

L_i = one-third octave band level of the i^{th} measurement

The results were labeled equivalent absolute spectra.

To compute the normalized energy average one-third spectra, each individual blast spectrum was first normalized by summing its bands on an energy basis and adjusting the levels so that the sum would equal 100 dB; this reduced the amplitude effects of individual blasts. For each of the 75 categories, these normalized blast data were then turned into a normalized energy average one-third octave spectrum for each frequency band, using Eq 5.

* Spectral analysis is possible for only two types of recorded data – good, clean blast signatures and data with slight noise present. These are the higher amplitude data necessary for community noise predictions rather than the less significant, low-level data.

$$Y = 10\log_{10}\frac{1}{n}\sum_{i=1}^{n}10^{LN_i/10} \qquad \text{[Eq 5]}$$

where n = number of blast measurements in a given category

LN_i = normalized one-third octave band level of the i^{th} measurement

Finally, the levels of the resulting spectra, labeled relative spectra, were adjusted so that the maximum reading in any frequency band would be 0 dB.

Following these computations, the differences between the spectra could be analyzed. The absolute spectra should be dominated by high amplitudes of individual blasts, whereas the relative spectra should be more reflective of the entire range of blasts.

To obtain these differences, the relative spectra had to be adjusted to the absolute spectra. This was accomplished by equating the relative spectra's equivalent frequency band readings to the maximum one-third octave band in the absolute spectra. In the example shown in Figure 23, the 31-Hz band in the absolute spectrum had a value of 90 dB and the equivalent 31-Hz band in the relative spectrum had a value of 0 dB. Adding 90 dB to each band in the relative spectrum and comparing it to the absolute spectrum produced the difference spectrum. It should be noted that a 1-dB rounding error occurred because of the increments used. Appendix D (Volume II) contains similar figures for all 75 categories.

The spectral peaks were generally in the range of 25 to 30 Hz. Since the theoretical signature near a 5-lb (2 kg) blast has an overall time duration of 30 msec, these observed frequencies correlated well with the original duration. Nevertheless, in many cases, large amounts of energy appeared around 10 to 15 Hz. A detailed examination of Figures 24 through 26 revealed that this effect was weather-dependent. These figures show the respective spectra for blast measurements lying in the focus, base, negative gradient, and excess negative gradient ranges. The data in each figure, aggregated over all distances and all stations for both day- and nighttime measurements, revealed the relationship between range and location of peak shown in Table 12.

Since the difference spectra for these four figures revealed little change between the absolute and relative spectra, these relations were universal and not dominated by the high amplitude data. Further examination of the data in Appendix D revealed this same trend for each individual distance.

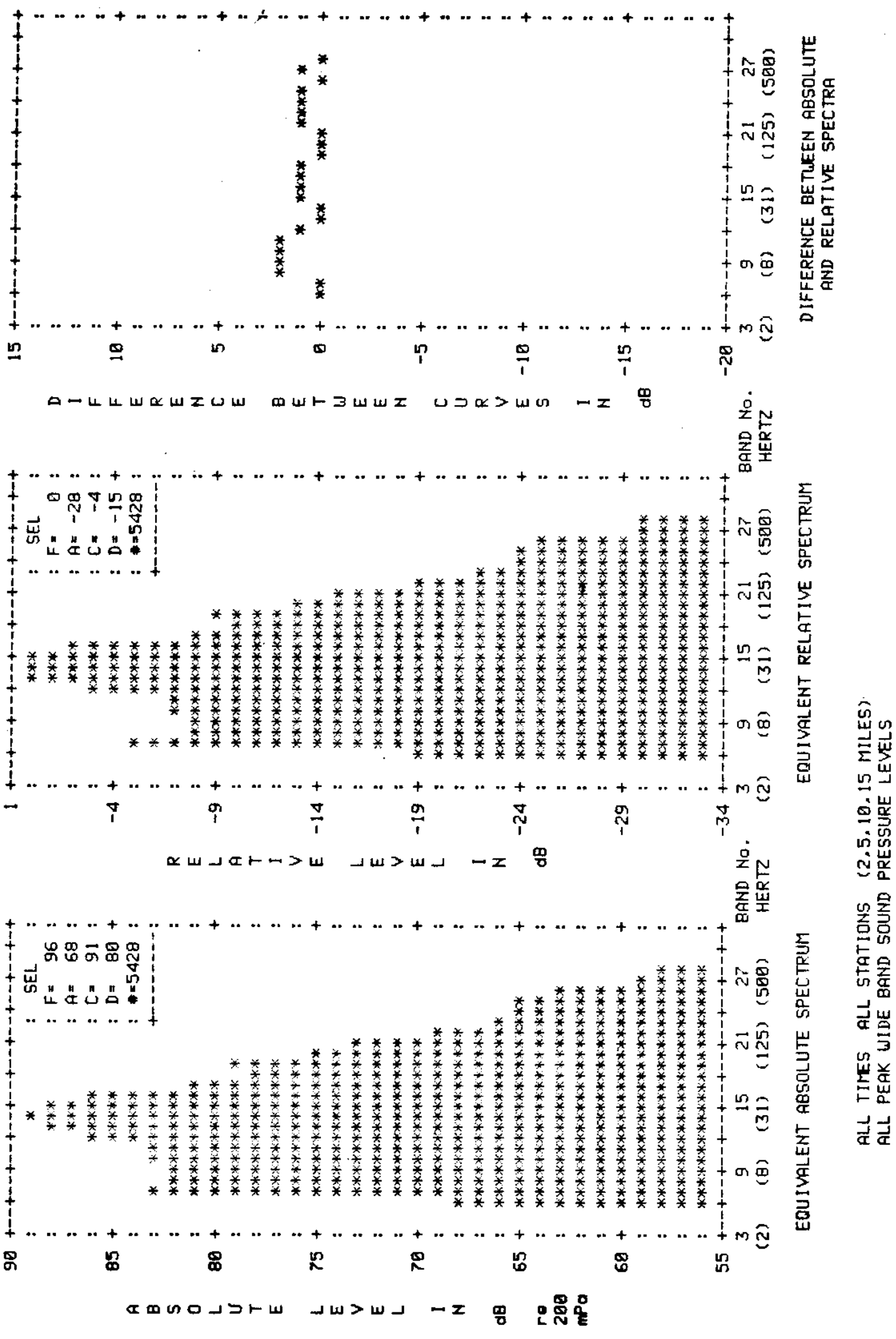

Figure 23. Comparison of absolute and relative one-third octave spectra.

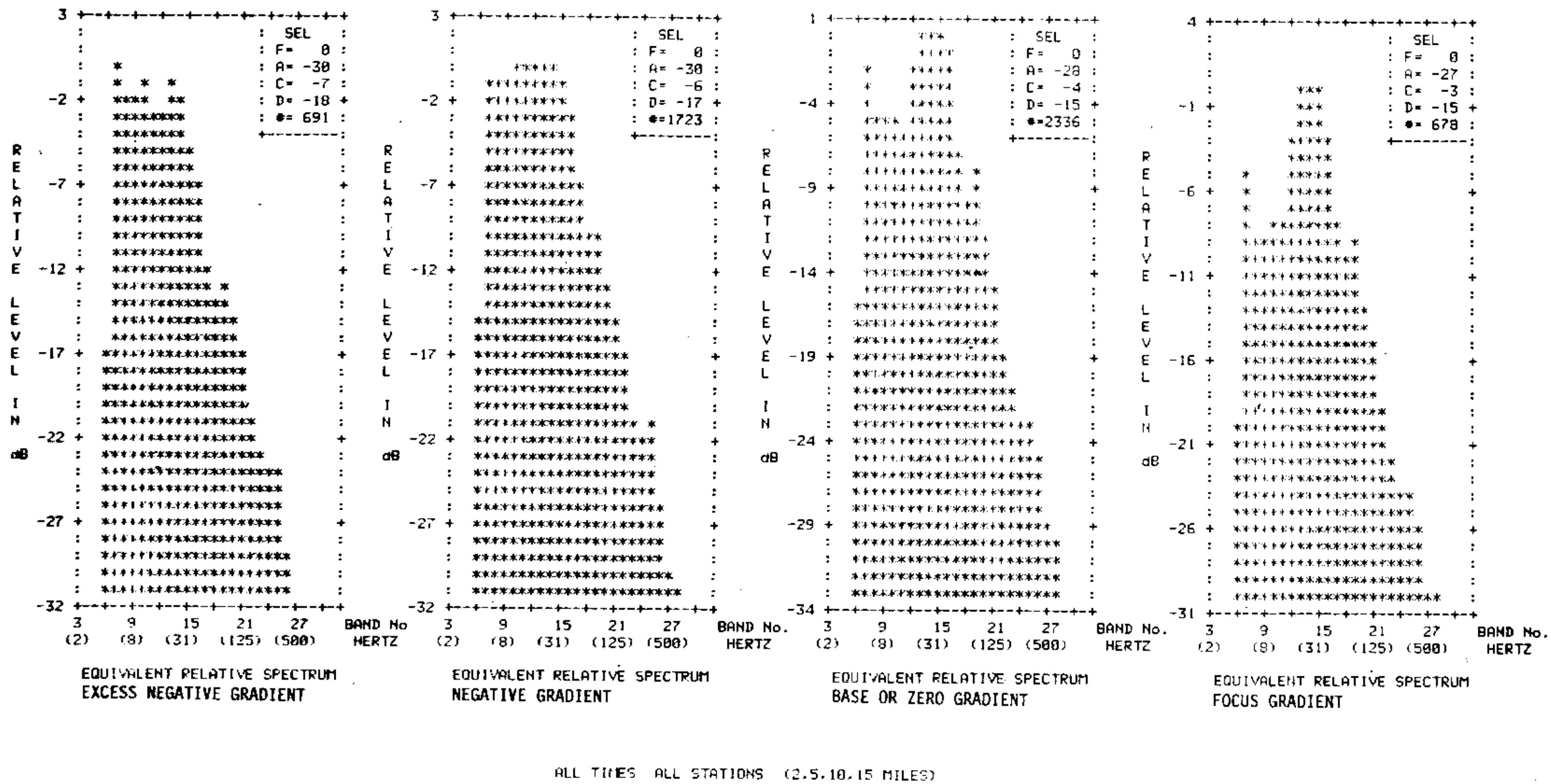

Figure 24. Comparison of absolute spectra to determine meteorological effects.

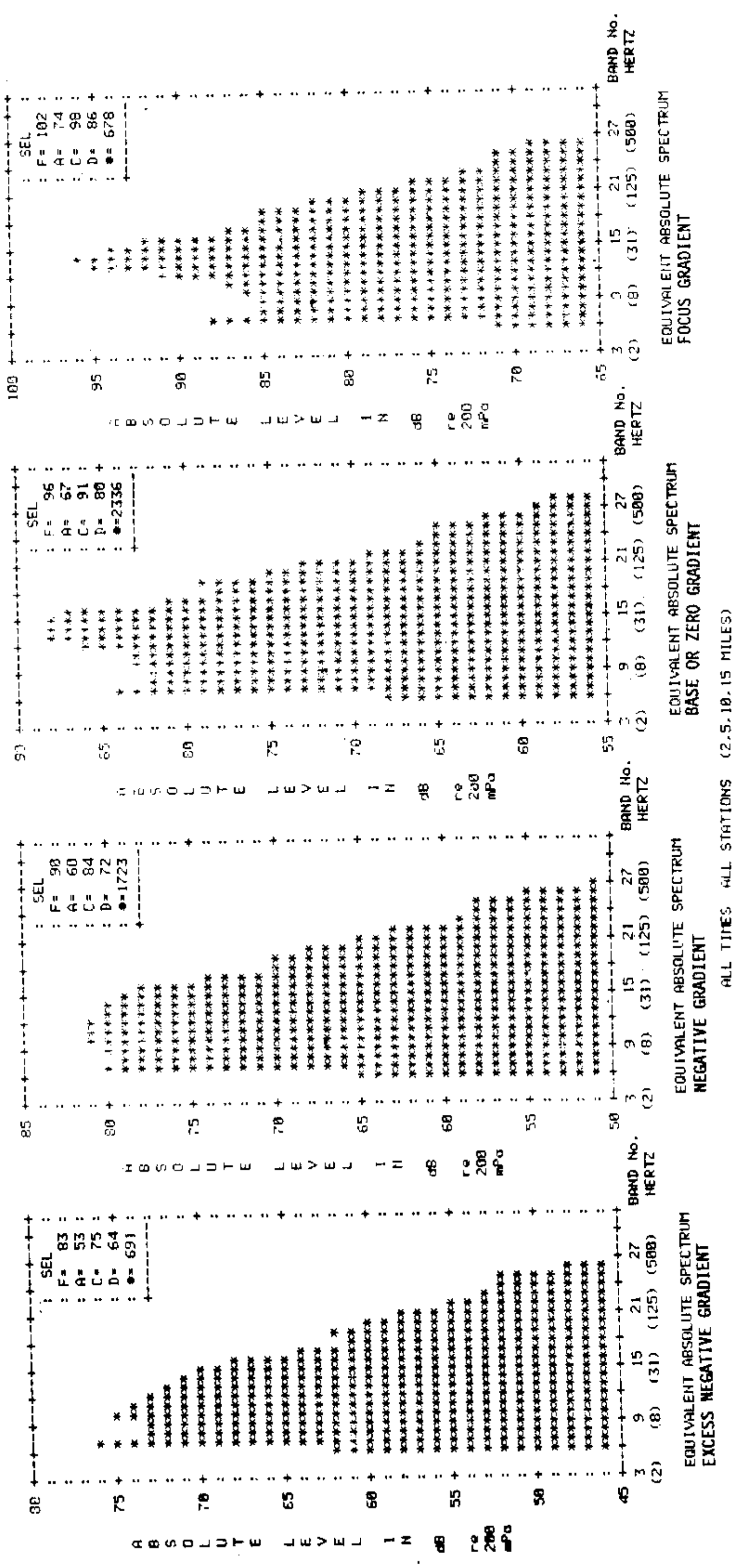

Figure 25. Comparison of relative spectra to determine meteorological effects.

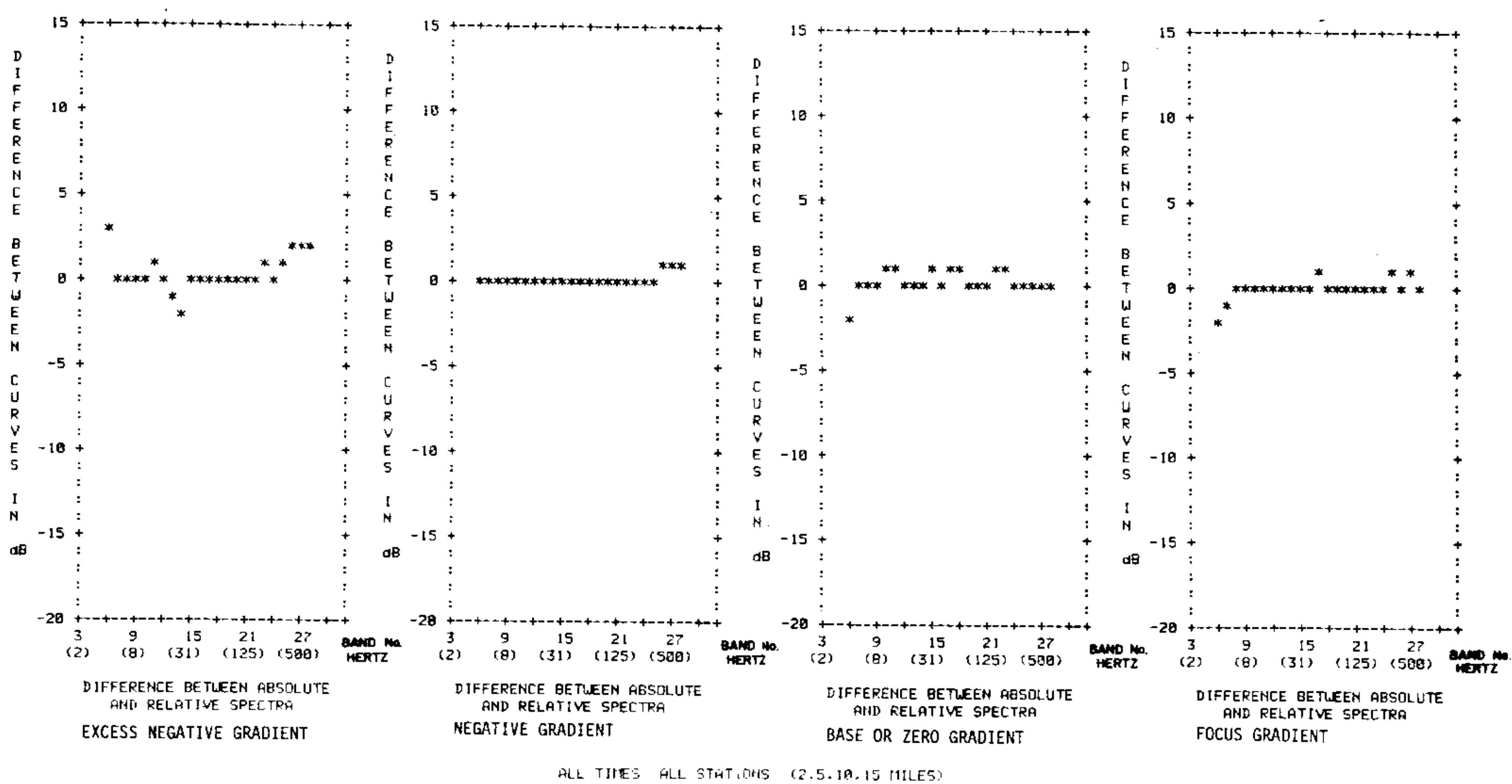

Figure 26. Comparison of difference spectra to determine meteorological effects.

Table 12. Relationship between range and location of peak.

Range	Result
Focus	Sharp peak at 25 to 30 Hz
Base	Broad peak at 25 to 30 Hz
Negative gradient	Broad, almost flat peak at 15 to 25 Hz
Excess negative gradient*	Peak at 10 to 15 Hz or less

* As discussed in Chapter 2, a 10-Hz pole was used to reduce the effects of wind on the data. The spectral peak at 10 to 15 Hz indicates that it could have attenuated some of the levels in this excess negative range by up to 5 dB. However, this amount does not itself account for this individual category.

Since each of the 2, 5, 10, and 15 mi (3, 8, 16, and 24 km) stations contained a significant number of data points, these results were not biased by one or two measurements.* Thus these data indicate a clear relationship between the resultant measured spectra and weather conditions independent of blast amplitude or distance.

Figure 27 illustrates how the apparent spectrum of a blast signal might change. Here, three identical N-waves out of time phase with each other were added to produce a totally dissimilar wave. The resulting wave clearly shows a shift in frequency content from high to low values. In reality, this condition would occur if the sound had to travel over multiple distinct paths somewhat different in length or in a continuum of different path lengths, thus arriving at an observation station at slightly different times.

These multi-paths did exist, especially in shadow zones and during negative gradient conditions where no direct sound path from source to receiver existed. Sound rays were refracted up during negative gradient conditions and over certain shadow zones during focus conditions. The measurements, which resulted from diffusion, can be visualized if a wave mode is employed for the sound propagation. All along the wave front one can think of different Huygens sources radiating or diffusing into the quiet zone.[9] Alternatively, from the ray viewpoint, the edges of the direct sound zones can represent caustics which continually radiate rays into the quiet zones according to geometric theories of diffraction.

* It should be noted that the 15-mi (24 km) stations contained fewer data points than the close-in stations. However, the number is still large enough so that the results were not biased by one or two measurements.

[9] I. Kay, "The Diffraction of an Arbitrary Pulse by a Wedge," *Comm. on Pure and Applied Mathematics,* Vol 6 (1953), pp 419-434.

An important use for the spectral data was the application of various weightings which could be correlated to a community response.* Appendix E (Volume II) contains five sets of data which relate various physical descriptors used for this purpose. These data sets include distributions of:

1. Peak wide-band sound pressure level minus A-weighted sound exposure level (Figure 28)
2. Peak wide-band sound pressure level minus C-weighted sound exposure level (Figure 29)
3. Flat-weighted sound exposure level minus A-weighted sound exposure level (Figure 30)
4. Flat-weighted sound exposure level minus C-weighted sound exposure level (Figure 31)
5. Peak wide-band sound pressure level minus flat-weighted sound exposure level (Figure 32).

Examination of Appendix E shows that the distributions were generally Gaussian in shape with a relatively small standard deviation. The exception occurred in Set 4 — the flat-weighted sound exposure level minus the C-weighted sound exposure level. This result was expected, however, since this difference can never be very large.

Set 2 is useful as input data in the current interim procedure for predicting community responses to impulse noise in the normal EPA L_{eq}/L_{dn} system, while Set 5 can be used to study the physics of sound propagation in the atmosphere. Sets 3 and 4 show the differences between various means of predicting community response to impulse noise.

* Applying the A-weighting curves to the one-third octave spectra produced the A-weighted SEL. Similar applications produced C-weighted and flat-weighted sound exposure levels.

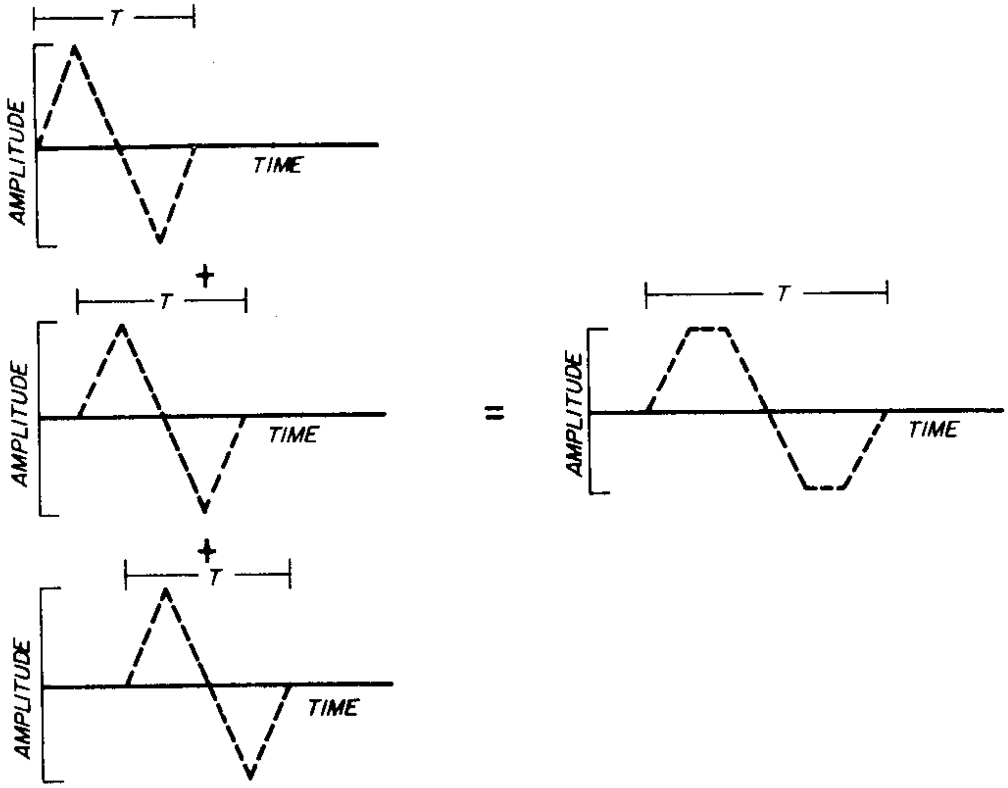

Figure 27. Time addition of out-of-phase N-waves.

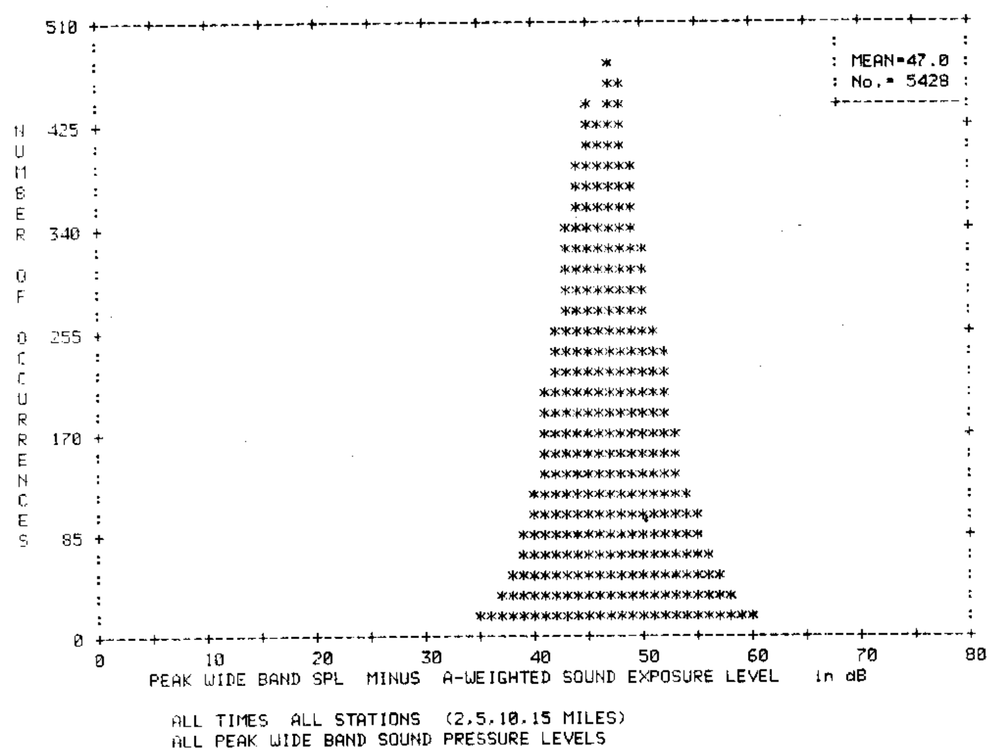

Figure 28. Peak wide-band sound pressure level minus A-weighted sound exposure level.

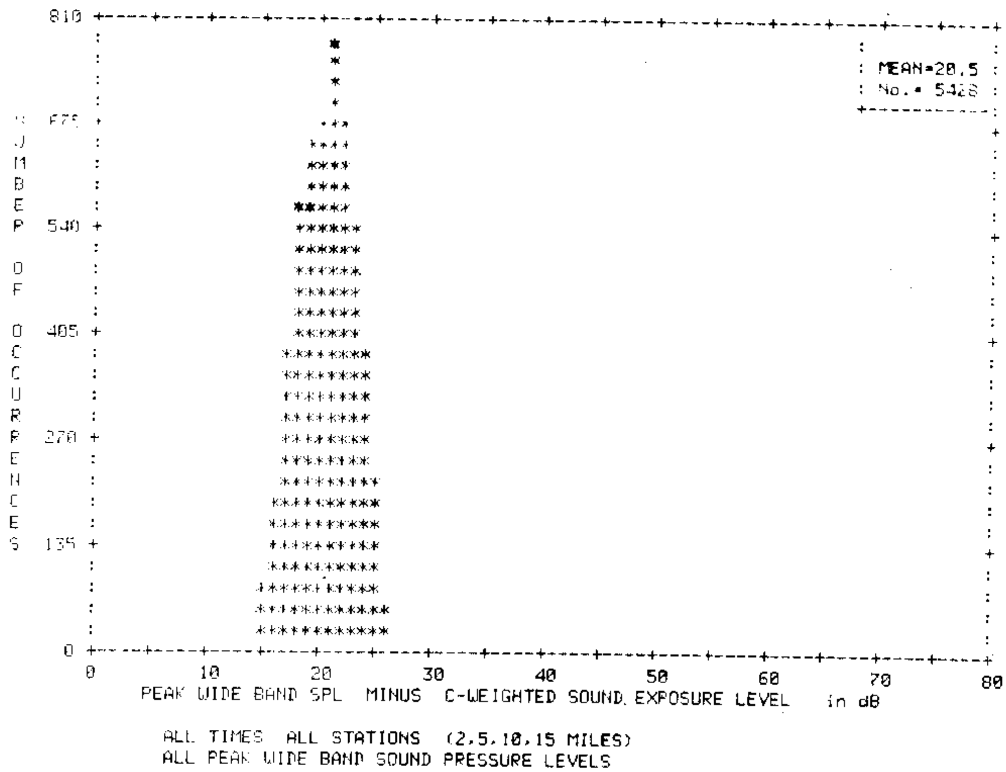

Figure 29. Peak wide-band sound pressure level minus C-weighted sound exposure level.

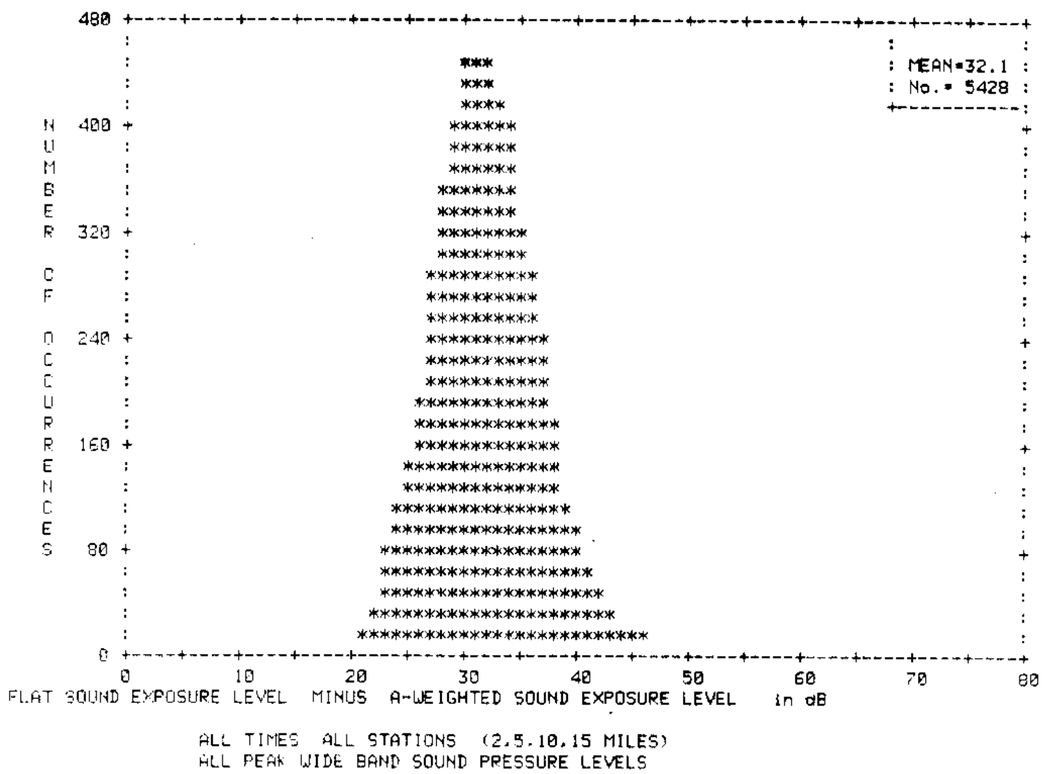

Figure 30. Flat-weighted sound exposure level minus A-weighted sound exposure level.

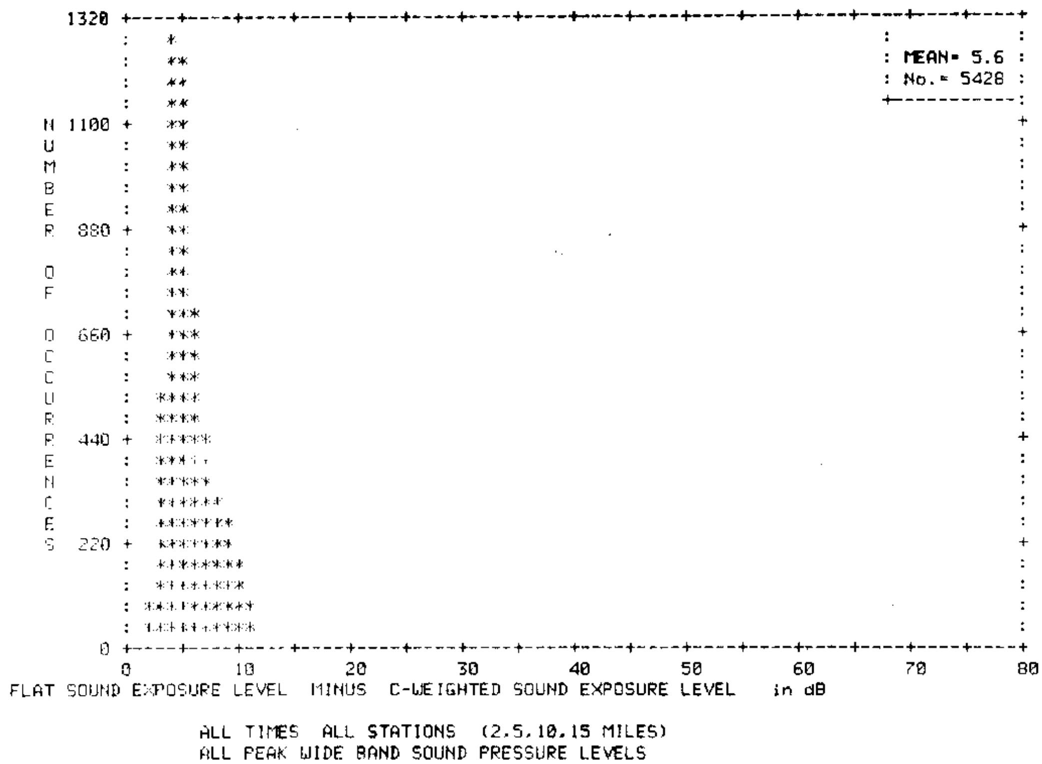

Figure 31. Flat-weighted sound exposure level minus C-weighted sound exposure level.

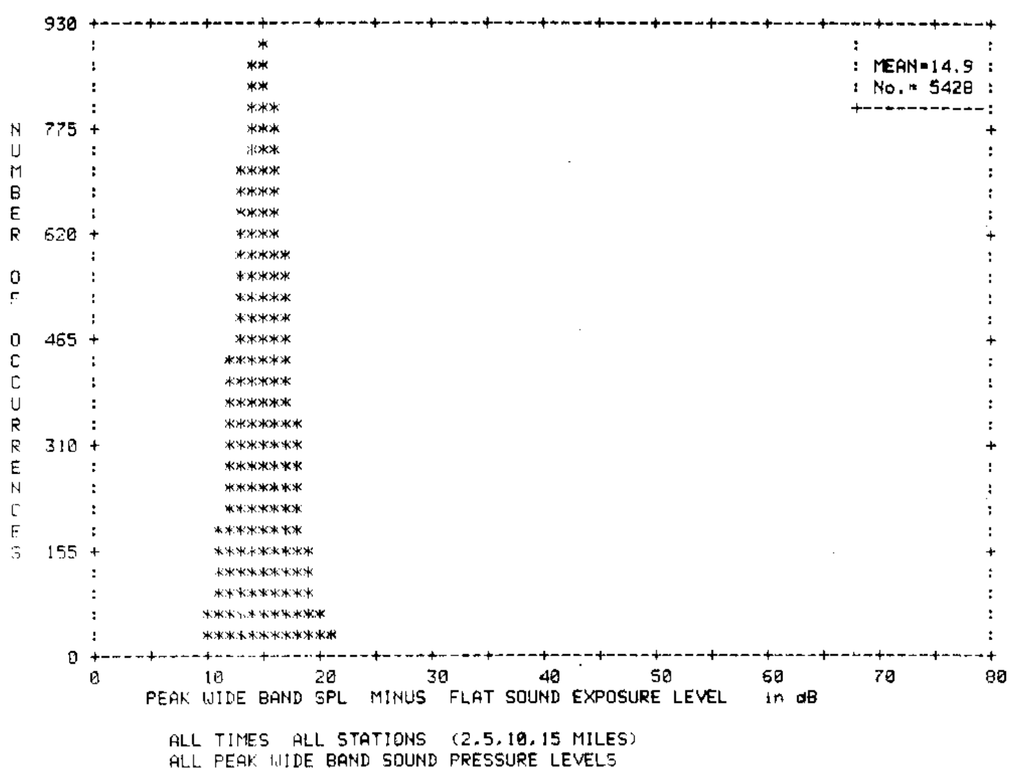

Figure 32. Peak wide-band sound pressure level minus flat-weighted sound exposure level.

8 Conclusions

The three main objectives of this study were achieved through (1) the development of blast propagation statistics of the measured data, (2) the establishment of a relationship between the specific meteorological and terrain conditions at Fort Leonard Wood and the measured blast amplitudes, and (3) the establishment of frequency-weighted one-third octave spectra for use in predicting community response to blast noise. The weather and terrain dependence implies that these data can be used to predict blast amplitudes under conditions similar to those at Fort Leonard Wood and to suggest plausible relationships between general weather conditions and blast statistics. Future studies will confirm these relationships for areas different from the Fort Leonard Wood area.

In addition, because of the scope of the Fort Leonard Wood study, many other conclusions were derived; they are presented according to the chapter in which they were developed.

Collection of Data (Chapter 2)

1. The procedure for recording blast data was simple enough so that nontechnical personnel could operate the equipment.

Data Analysis (Chapter 3)

2. The one-third octave spectra obtained with narrow-band analysis were, within the limits of measure, identical to spectra obtained with a one-third octave filter.

3. Although the calibration signal could not be played through the narrow-band analyzer, absolute values of the spectra could be obtained by calculating the integral of the time varying signal squared, $\int_0^t p^2(t)dt$. This pressure-squared integral could be derived by using time-consuming digital analysis. However, from a sample of the data, a curve was established relating this value to peak and impulsive levels. The pressure-squared integrals for the remaining data could be derived from this curve.

Statistics of Blast Propagation in the Atmosphere (Chapter 4)

4. Amplitude distributions of blast data based on time and distance were divided into four ranges by natural breaks. The statistics of blast propagation were developed by determining the percentage of blast amplitudes within each range. Amplitude versus distance curves could be graphed from the energy average amplitudes in each range.

Comparison of the Blast Propagation Statistics to Theoretical Amplitude Distance Prediction Curves (Chapter 5)

5. The amplitude versus distance curves compared quite closely with the theoretical prediction curves in CERL Technical Report E-17.[10] Since these prediction curves were based on meteorological conditions, a weather dependence was implied for the Fort Leonard Wood data.

6. The maximum probable focus curve, established in CERL Technical Report E-17 to protect against structural damage and other extremes, was verified.

The Effect of Weather and Terrain on Blast Noise Prediction (Chapter 6)

7. For subsequent studies, weather data at more frequent time and distance intervals are desirable.

8. Approximately 66.0 percent of the individual blast amplitudes fell within 7 dB of predictions based on the amplitude versus distance curves developed in Chapter 4 and on the available meteorological data. Of the remaining disagreement data, 15.7 percent could be physically explained while 10.7 percent could be correlated to a specific set of meteorological conditions. Only 7.6 percent were unexplained. Most of the disagreement data fell below the predicted results. The physical explanation and correlations listed in Table 6 give reliable trends for the disagreement data.

---

[10] P. D. Schomer, *Predicting Community Response to Blast Noise,* Technical Report E-17/AD773690 (CERL, 1973).

9. For some stations, the terrain prevented a direct line of sight to the blast site. If the measurements affected by barriers are eliminated from the analysis, the agreement percentage increases to 70.5, while the unexplained percentage drops to 5.4 percent. These figures verify the weather dependence implied in Chapter 5.

10. At shorter distances and toward the end of the day, the largest amplitudes were measured downwind. At further distances and early in the day, the largest amplitudes occurred upwind.

Spectral Contents of Blast Noise (Chapter 7)

11. Use of normalized spectra negates the effects of individual large amplitude blasts on the data.

12. The spectral peak of blasts usually occurred between 25 and 30 Hz, although weather conditions sometimes shifted this peak to 15 Hz.

13. By applying different frequency weightings to these spectra to form various weighted sound exposure levels, the blast data can be used to compute some community response measures.

References

Homans, B., J. McBryan, and P. Schomer, *User Manual for the Acquisition and Evaluation of Operational Blast Noise Data*, Technical Report E-42/AD782911 (U. S. Army Construction Engineering Research Laboratory [CERL], 1974).

Information on Levels of Environmental Noise Requisite to Protect Public Health and Welfare With an Adequate Margin of Safety, EPA 550/9-74-004 (Environmental Protection Agency, March 1974).

Kay, I., “The Diffraction of an Arbitrary Pulse by a Wedge,” *Comm. on Pure and Applied Mathematics*, Vol 6 (1953).

Perkins, B., Jr., P. H. Lorrain, and W. H. Townsand, *Forecasting the Focus of Air Blast Due to Meteorological Conditions in the Lower Atmosphere*, Report No. 1118 (Ballistics Research Laboratories, 1960).

Reed, J. W., *Acoustic Wave Effects Project: Airblast Prediction Techniques*, Report SC-M-69-332 (Sandia Laboratories, 1969).

Schomer, P. D., *Predicting Community Response to Blast Noise*, Technical Report E-17/AD773690 (CERL, 1973).

Thompson, R. S., *Computing Sound Ray Paths in the Presence of Wind*, Report SC-RR-67-53 (Sandia Laboratories, 1967).

Appendix A: Meteorological Data

Table A1 lists the meteorological measurements for the Fort Leonard Wood study and the slopes of the corresponding sound velocity gradients. Columns 1 and 2 list the dates and times of the wind flights by the FAA instrument plane. Column 3 gives turbulence, rated between 0 and 10 under the Universal Indicated Turbulence System (UITS). The values in columns 4 through 7 are wind speed and direction which were obtained at ground level from the Fort Leonard Wood weather station and at upper altitudes (1000, 2000, and 3000 ft [305, 610, and 914 m] AGL) for appropriate sensors in the FAA instrument package. The speed is given in knots and the directions in degrees, with 0 representing wind coming from the north, 90 from the east, 180 from the south, and 270 from the west. Column 8 lists the blasts which are temporally related to these meteorological conditions.

From this information, sound velocity gradient profiles were created in the north, south, east, and west directions from the source (Column 9). These profiles were linearized with the slopes of their straight segment approximations listed in Columns 10 through 15. The units of the slopes are ft/sec/ft (m/sec/m) and the column headings 1st, 2nd, 3rd, etc., refer to the straight-line segment in the profile beginning with the segment closest to the ground. More slope values are given if more segments were required to approximate the curve.

Table A1. Meteorological data.

Wind (knots – direction)									Total Gradient (ft/sec/ft or m/sec/m)					
Date	Time of Wind Run	Turb	Grnd	1000	2000	3000	Blast #	Dir	1st	2nd	3rd	4th	5th	6th
6-11	0540	4.0	2-190	32-258	18-215	23-215	36-40	N	.059	.000	-.047	.010		
								E	.075	-.037	-.005			
								S	-.027	.023	-.019			
								W	-.019	-.070	.023	-.010		
6-11	0540	4.0	2-190	32-258	18-215	23-215	41-45	N	.075	-.005	.007			
								E	.075	-.039				
								S	-.059	.010	-.016			
								W	-.039	-.075	.033	-.010		

Wind (knots – direction)									Total Gradient (ft/sec/ft or m/sec/m)					
Date	Time of Wind Run	Turb	Grnd	1000	2000	3000	Blast #	Dir	1st	2nd	3rd	4th	5th	6th
6-11	0629	3.6	3-195	33-265	17-210	38-266	46-49	N	.155	.023	-.047	.016	-.033	
								E	.075	-.023				
								S	-.033	.047	-.023	.016		
								W	-.027	-.059				
6-11	0629	3.6	3-195	33-265	17-210	38-266	50-54	N	.047	.007	-.037	.033		
								E	.047	.155	-.047	.039		
								S	-.027	.027	-.039	-.007	.016	
								W	-.033	-.075	.033			
6-11	0716	4.0	3-200	18-247	27-261	27-259	55-58	N	.039	.010	-.010	.000		
								E	.039	.013	-.010			
								S	-.005	.000	.005	-.007		
								W	-.005	-.039				
6-11	0716	4.0	3-200	18-247	27-261	27-259	59-61	N	.027	-.010	-.005			
								E	.023	.039	.010	-.005		
								S	-.010	.010	-.005			
								W	-.016	-.033				
6-11	0915	4.8	6-240	15-231	11-224	*	89-95	N	.010	.027	-.010			
								E	-.016	.007	-.013			
								S	-.033	.000				
								W	-.023	-.010				
6-12	0629	4.4	4-210	42-273	30-262	26-275	109-112	N	.115	.016	-.059	.007		
								E	.075	-.023				
								S	-.027	.059	-.010			
								W	-.027	-.102				
6-12	0629	4.4	4-210	42-273	30-262	26-275	113-118	N	.019	-.023	.010			
								E	.059	.075	-.033			
								S	-.019	.039	-.005			
								W	-.075	.010				
6-12	0845	5.6	8-290	29-279	14-259	25-268	127-137	N	-.016	-.023	.059	.007		
								E	.033	.047	.027	-.027	.016	
								S	-.033	.005	.013	-.016		
								W	-.075	-.047	.023	-.023		
6-12	0845	5.6	8-290	29-279	14-259	25-268	138-148	N	-.010	.019	.007			
								E	.023	.047	-.020	.016		
								S	-.005	-.013				
								W	-.059	.033	-.033			
6-12	0946	6.0	6-300	7-297	27-279	23-280	150-154	N	-.010	.000	-.013	.005		
								E	-.010	.033	-.007			
								S	-.016	-.010	.010			
								W	-.016	-.007	-.047	.007		

* No data obtained in this category.

Wind (knots – direction)									Total Gradient (ft/sec/ft or m/sec/m)					
Date	Time of Wind Run	Turb	Grnd	1000	2000	3000	Blast #	Dir	1st	2nd	3rd	4th	5th	6th
6-13	0544	3.0	4-004	16-027	21-306	*	155-156	N	.059	-.059	-.010	.016		
								E	-.010	.050	.019			
								S	-.047	.060	.016	-.017		
								W	.033	.005	-.047			
6-13	0706	3.8	3-007	15-086	21-292	11-287	169-170	N	-.030	.060	-.075	.016		
								E	.045	-.075	.060	-.023		
								S	.047	-.059	.060	-.016		
								W	-.047	.075	-.059	.010		
6-13	0923	4.0	3-150	8-081	5-210	29-283	196-198	N	-.027	.027	-.033	.019		
								E	.027	-.047	.027	.039		
								S	-.016	.047	-.033			
								W	-.047	.033	-.047	-.010		
6-13	0923	4.0	3-150	8-081	5-210	29-283	199-201	N	-.016	.023	-.033			
								E	.016	-.027	.033	-.005		
								S	-.019	.013	-.027			
								W	-.039	.023	-.039			
6-14	0808	3.6	5-130	16-212	10-198	28-114	242-244	N	.016	.075	.010	-.007		
								E	-.016	.039	-.010			
								S	-.039	-.016	.002			
								W	-.007	-.039	.005			
6-14	0808	3.6	5-130	10-198	28-114	28-114	245-248	N	.033	.059	-.010			
								E	.005	-.019	.047	-.019		
								S	-.039	-.005	.002			
								W	-.019	.005	.047			
6-14	1012	5.2	4-160	9-210	6-210	12-174	265-270	N	.000	-.016	.033	-.005		
								E	.002	-.016	.033	-.005		
								S	-.013	.033	.000	-.016		
								W	-.019	.033	.000	.010		
6-14	1012	5.2	4-160	9-210	6-210	12-174	271-280	N	-.016	.007	-.007			
								E	-.033	.013	-.015	-.013		
								S	-.059	-.013	.000	-.016		
								W	.019	.000	.005			
6-15	0835	6.0	11-220	28-262	33-214	44-270	281-282	N	-.016	.047	-.047			
								E	.047	-.016	.047			
								S	-.010	.013	-.039			
								W	-.047	.016	-.047			
6-19	0728	4.4	6-140	16-208	35-219	40-230	309-315	N	.016	.023	-.010			
								E	.000	.039	.023	.033	.013	
								S	-.033	-.023	.016	-.023		
								W	-.016	-.039	-.016			

* No data obtained in this category.

Wind (knots – direction)									Total Gradient (ft/sec/ft or m/sec/m)					
Date	Time of Wind Run	Turb	Grnd	1000	2000	3000	Blast #	Dir	1st	2nd	3rd	4th	5th	6th
6-19	0945	5.2	6-140	43-022	37-035	36-046	336-345	N	-.059	-.102	.013			
								E	-.075	.019	-.010			
								S	.039	.102	-.023			
								W	.059	-.023	.005			
6-19	0945	5.2	6-140	43-022	37-035	36-046	346-349	N	-.102	.013	.010			
								E	-.027	-.016	.010	-.013		
								S	.075	-.023	-.010			
								W	.016	.010				
6-20	0622	4.0	CALM	8-266	20-332	20-342	366-372	N	.016	.033	-.005	-.003		
								E	.039	.005	-.002			
								S	.040	.010	.023	-.005		
								W	.033	-.023	-.016			
6-20	0622	4.0	CALM	8-286	20-332	20-342	373-384	N	.047	-.016	-.033			
								E	.033	.007	-.007			
								S	.023	.005	.023	-.002		
								W	.023	-.019	.002			
6-20	0805	6.0	4-240	22-226	23-247	22-246	390-392	N	.039	.019	-.016			
								E	.047	.016	-.016			
								S	-.016	-.030	.005			
								W	-.033	-.007				
6-20	0805	6.0	4-240	22-226	23-247	22-246	393-395	N	.039	.019	-.016			
								E	.047	.016	-.016			
								S	-.016	-.030	.005			
								W	-.003	-.007				
6-20	0957	6.2	3-250	16-266	29-246	24-274	398-405	N	.000	-.013	-.013	-.027		
								E	.023	.016	-.007			
								S	-.010	.005	-.023			
								W	-.033	-.027	-.005			
6-20	0957	6.2	3-250	16-266	29-246	24-274	406-410	N	-.007	.013	-.027			
								E	.075	.023	.030	.016	-.010	
								S	-.023	.016	-.023	.019		
								W	-.033	-.027				
6-20	0957	6.2	3-250	16-266	29-246	24-274	411-416	N	-.007	.013	-.027			
								E	.075	.023	.030	.016	-.010	
								S	-.023	.016	-.023	.019		
								W	-.033	-.023				
6-21	0858	5.8	5-230	12-310	15-305	20-312	473-479	N	-.023	-.027	-.002			
								E	.016	.000	-.002			
								S	.000	.020	-.002	.016		
								W	-.033	.013				

Wind (knots – direction)									Total Gradient (ft/sec/ft or m/sec/m)					
Date	Time of Wind Run	Turb	Grnd	1000	2000	3000	Blast #	Dir	1st	2nd	3rd	4th	5th	6th
6-21	0858	5.8	5-230	12-310	15-305	20-312	480-482	N	-.023	-.019	-.027			
								E	.000	.016	.000	-.013		
								S	-.016	.027	-.016			
								W	-.039	-.016	-.023			
6-22	0552	1.4	CALM	*	11-322	15-314	507-511	N	.023	-.005	-.023			
								E	.033	.016	.002	-.010		
								S	.013	-.005				
								W	-.016	-.013				
6-22	0552	1.4	CALM	*	11-322	15-314	512-520	N	.023	-.005	-.023			
								E	.033	.016	.002	-.010		
								S	.013	-.005				
								W	-.016	-.013				
6-22	0935	5.2	7-310	12-308	14-323	17-337	555-562	N	-.033	-.016				
								E	-.010	.010	-.005			
								S	-.002	.010				
								W	-.033	.007				
6-25	*	3.0	4-175	9-197	12-245	15-273	*	N	*	*	*	*	*	*
								E	*	*	*	*	*	*
								S	*	*	*	*	*	*
								W	*	*	*	*	*	*
6-26	*	7.4	7-240	18-241	22-251	22-264	*	N	*	*	*	*	*	*
								E	*	*	*	*	*	*
								S	*	*	*	*	*	*
								W	*	*	*	*	*	*
6-26	*	5.5	10-240	18-252	25-264	25-282	*	N	*	*	*	*	*	*
								E	*	*	*	*	*	*
								S	*	*	*	*	*	*
								W	*	*	*	*	*	*
6-27	*	5.0	4-270	10-242	15-254	19-261	*	N	*	*	*	*	*	*
								E	*	*	*	*	*	*
								S	*	*	*	*	*	*
								W	*	*	*	*	*	*

* No data obtained in this category.

Appendix B: Amplitude Distributions

The blast data in Chapter 3 were divided into five categories: (1) good, clean blast signatures, (2) data with slight noise present, (3) data containing significant noise, but for which there is an accurate measure of the peak value, (4) data for which the peak value could only be estimated, and (5) data missed because of equipment failures or calibration during an event.

Using the first three categories, peak sound pressure level distributions were created based on the four distances (2, 5, 10, and 15 mi [3, 8, 16, and 24 km]) and two time periods (0500 to 0700 hours and 0700 to 1100 hours). Figures B1 through B8 illustrate these eight distributions. As these figures show, each distribution could be subdivided into four ranges using three natural breaks. Table B1 lists the initial and adjusted final breakpoint values, which are indicated in the figures by arrows and dashed vertical lines, respectively. Table B2 shows the extension of values for each of the resulting ranges.

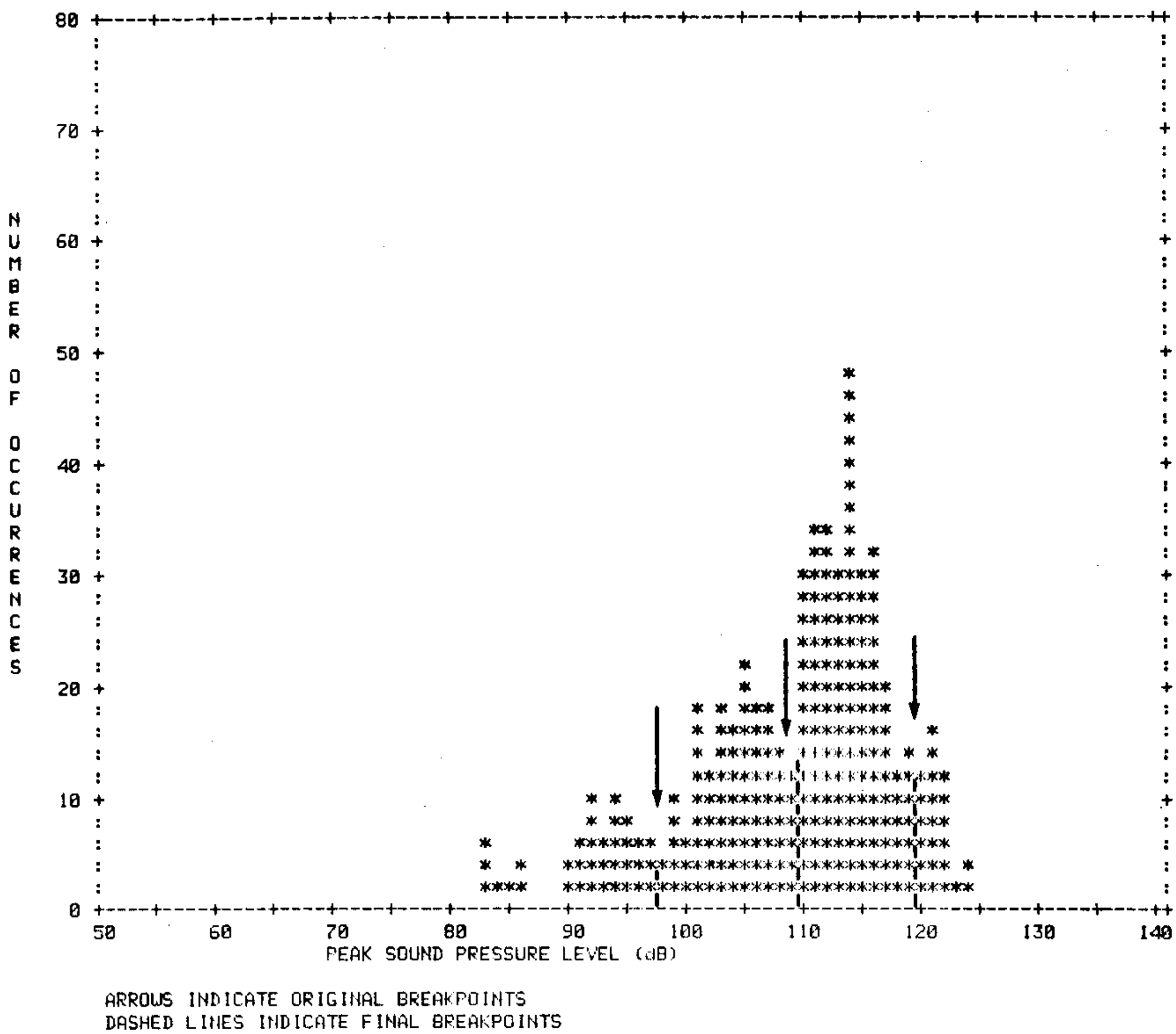

Figure B1. Two-mi nighttime peak sound pressure level distribution (original and final breakpoints).

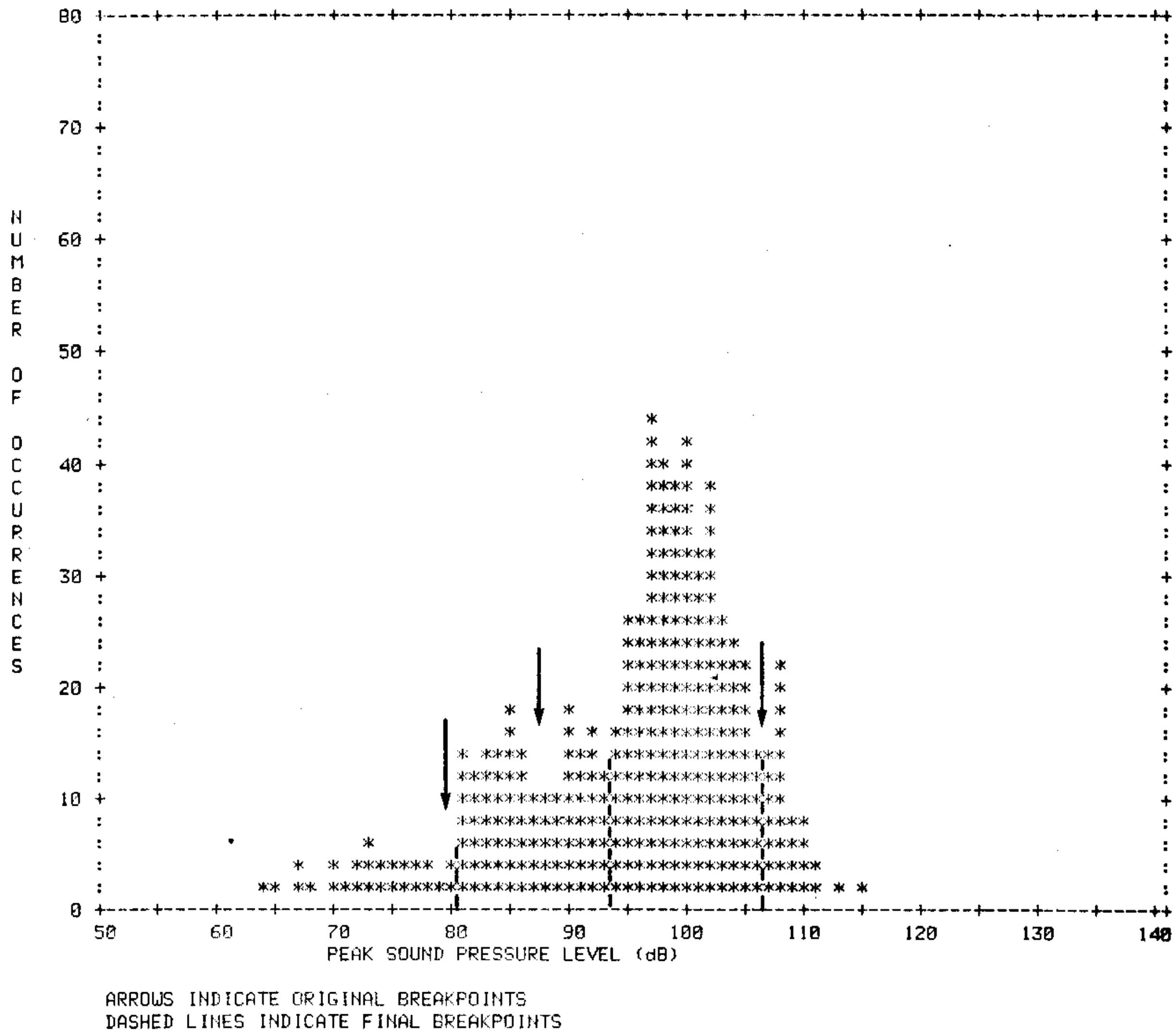

Figure B2. Five-mi nighttime peak sound pressure level distribution (original and final breakpoints).

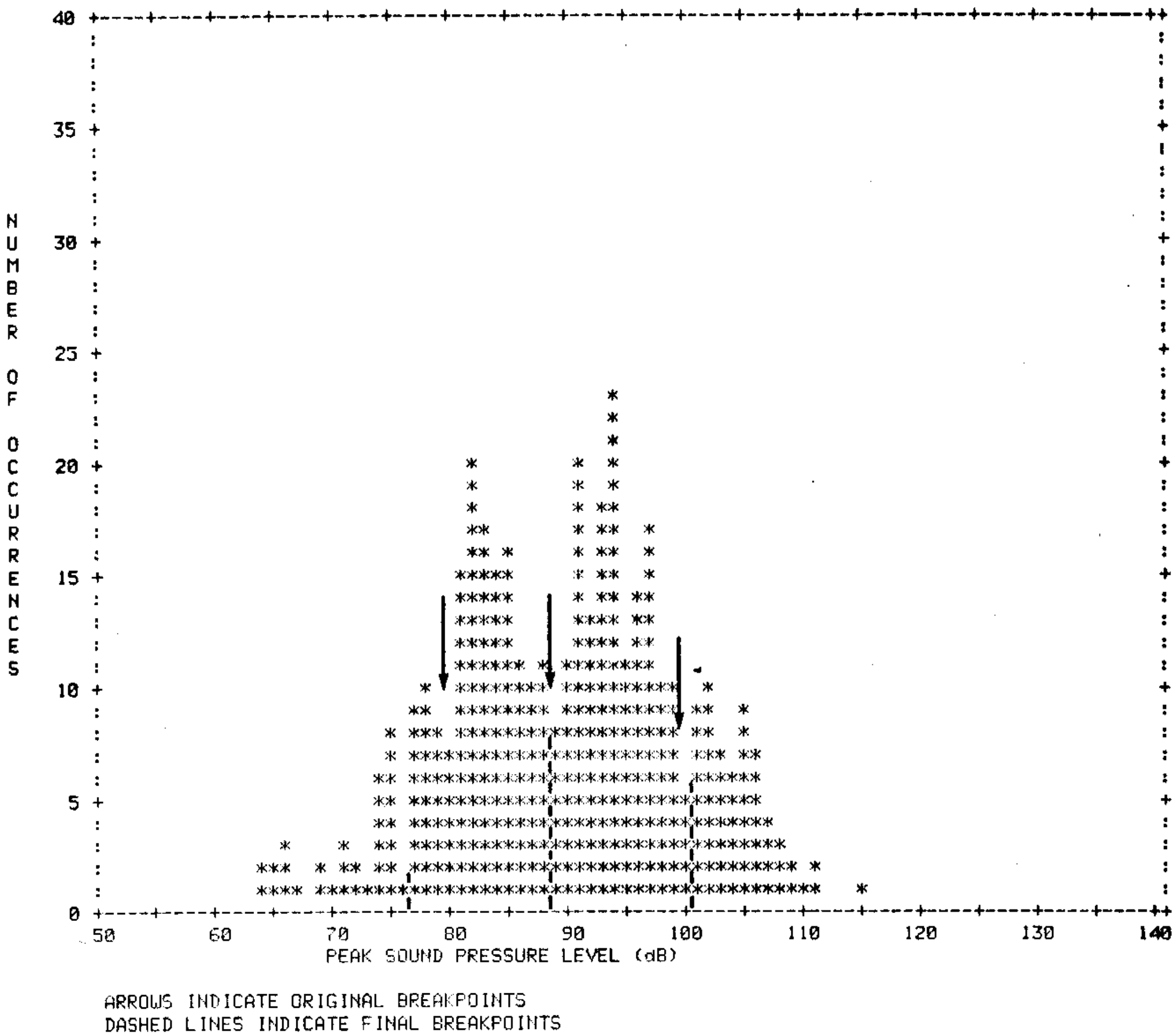

Figure B3. Ten-mi nighttime peak sound pressure level distribution (original and final breakpoints).

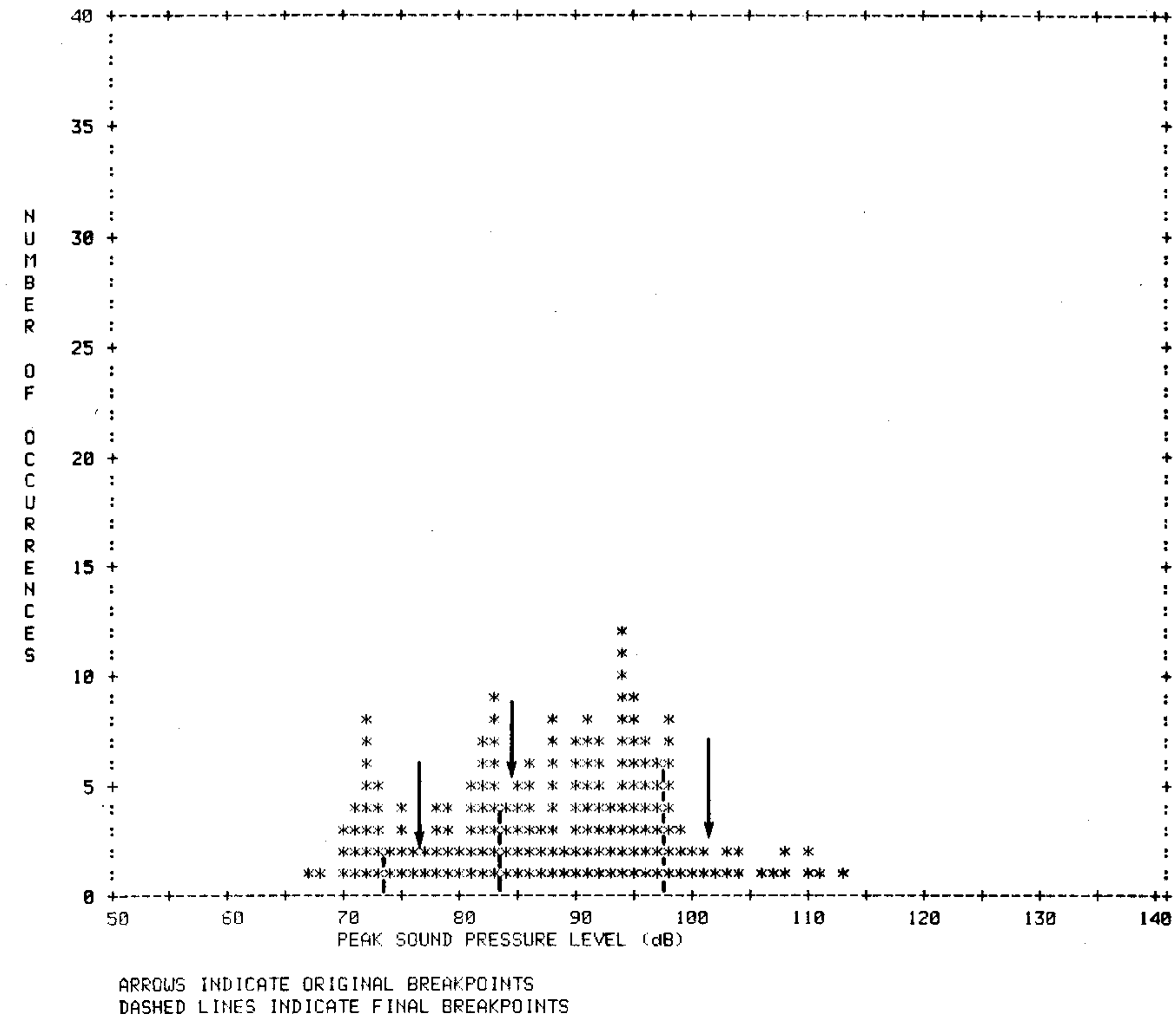

Figure B4. Fifteen-mi nighttime peak sound pressure level distribution (original and final breakpoints).

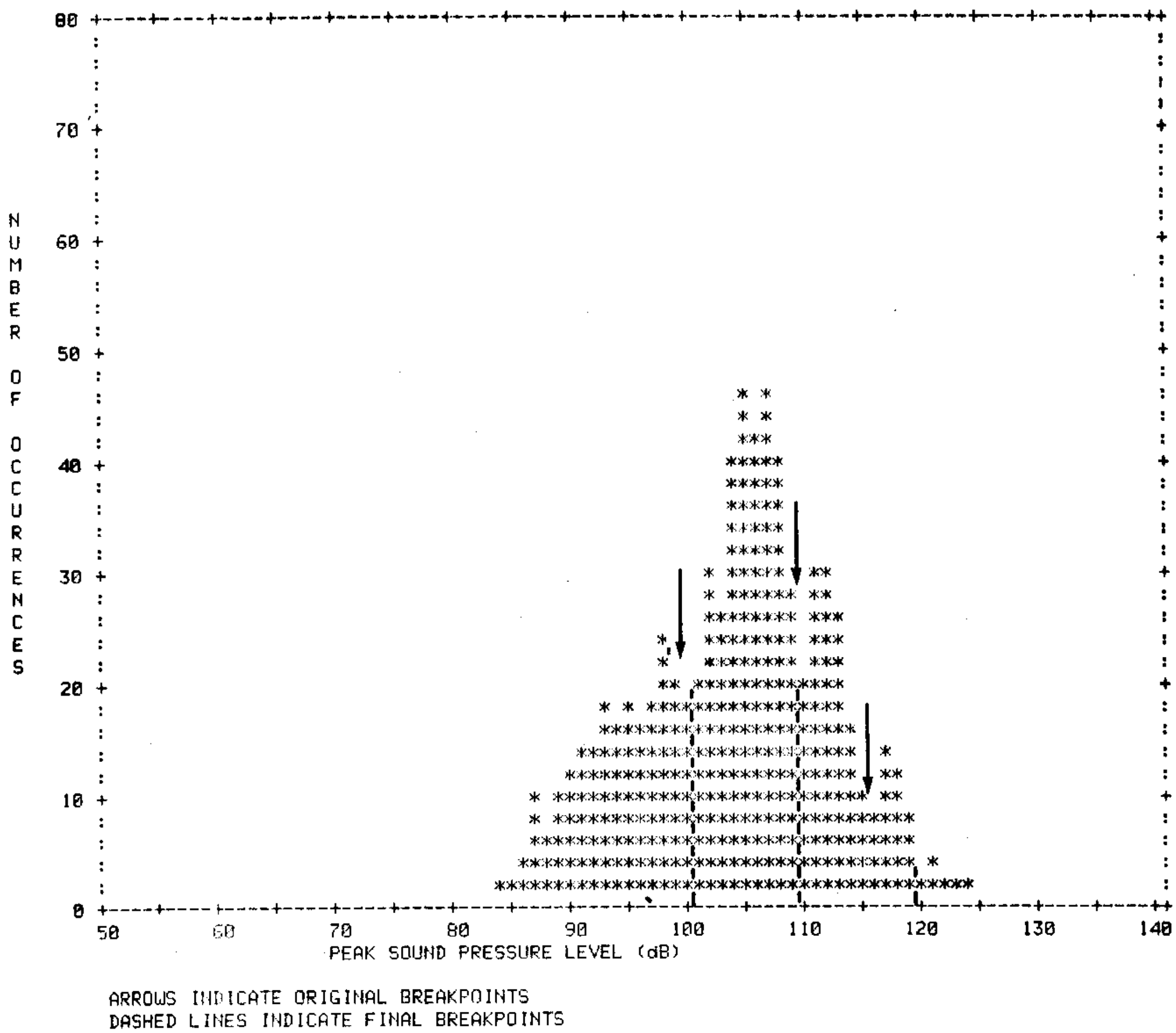

Figure B5. Two-mi daytime peak sound pressure level distribution (original and final breakpoints).

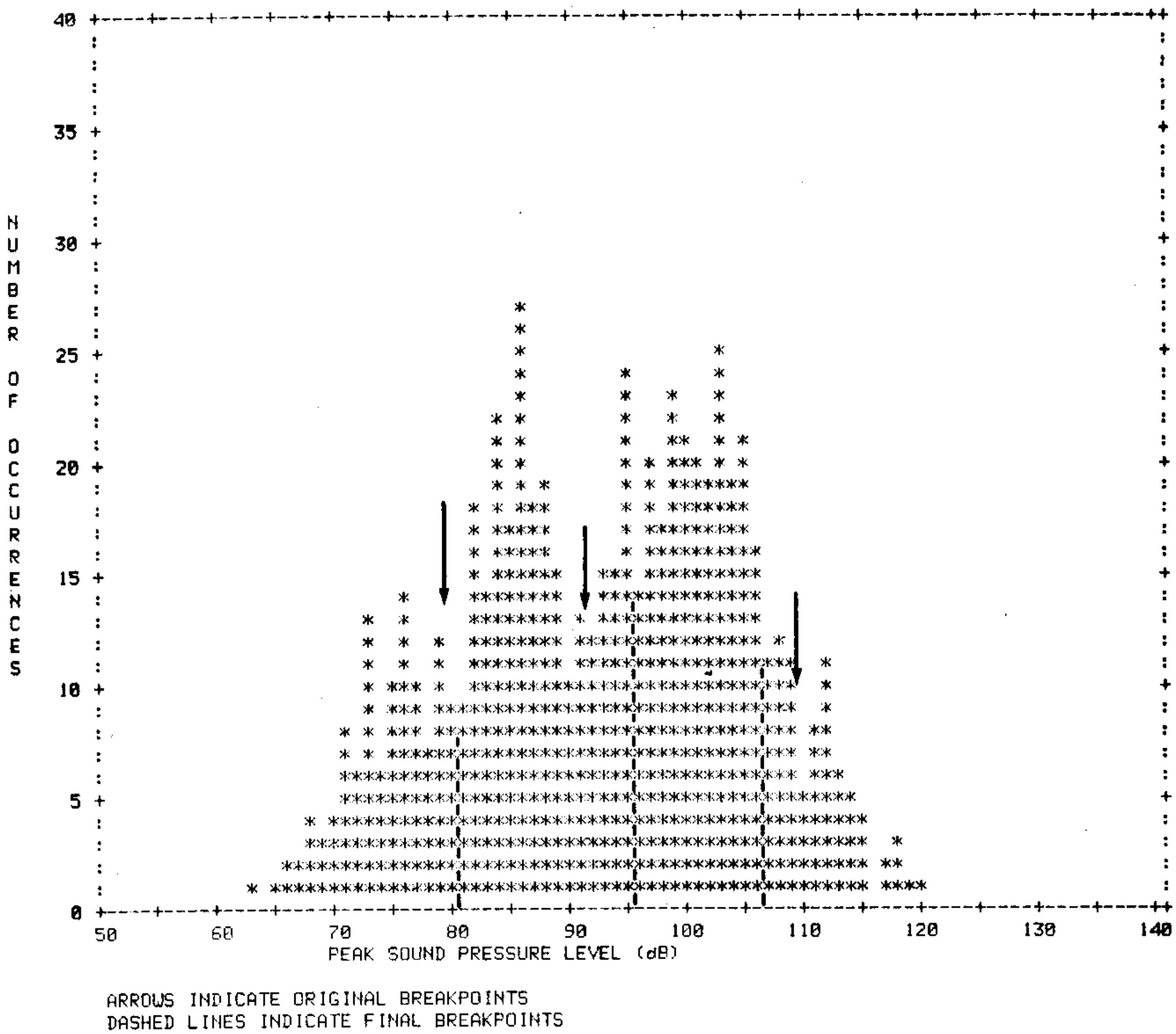

Figure B6. Five-mi daytime peak sound pressure level distribution (original and final breakpoints).

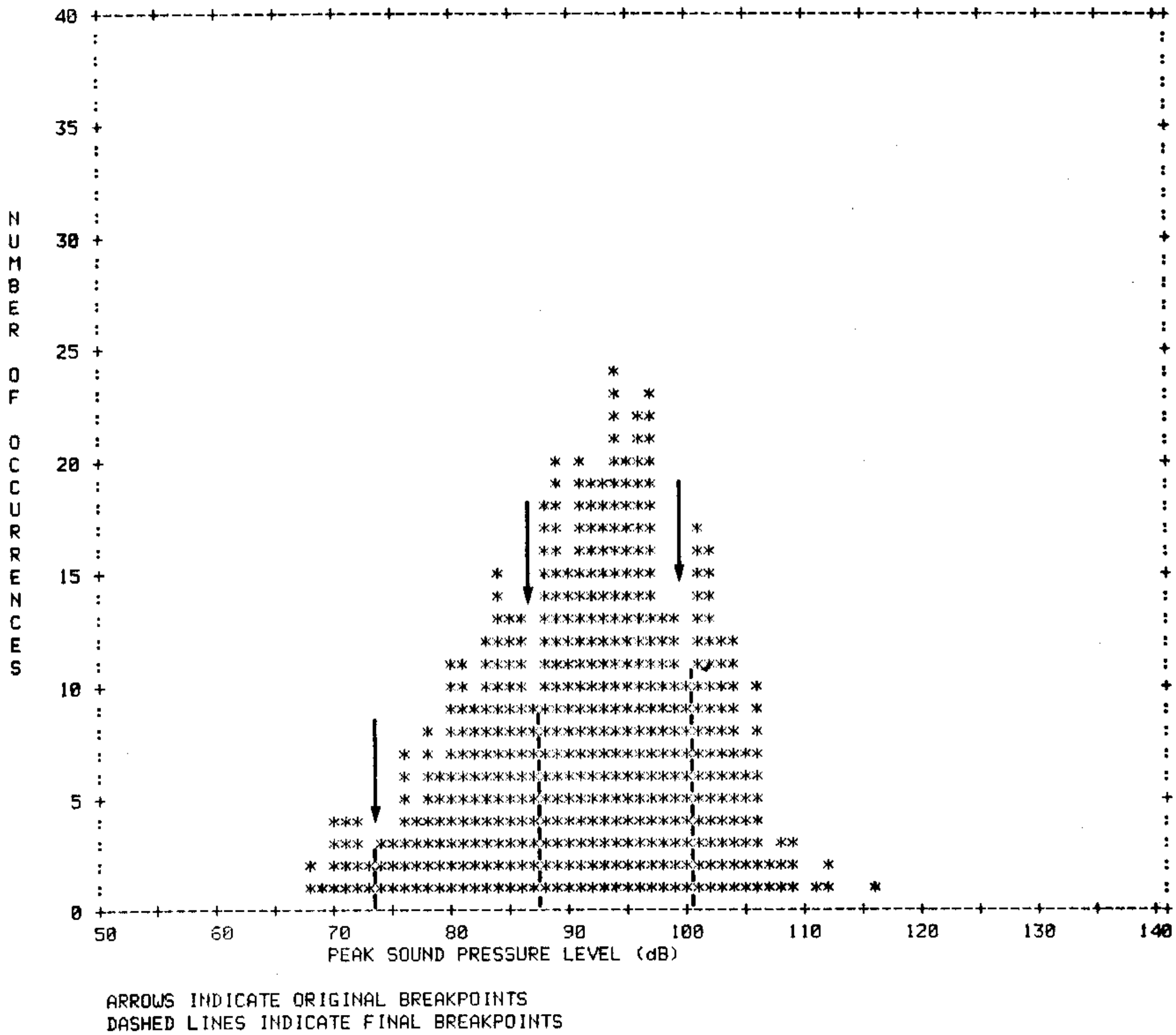

Figure B7. Ten-mi daytime peak sound pressure level distribution (original and final breakpoints).

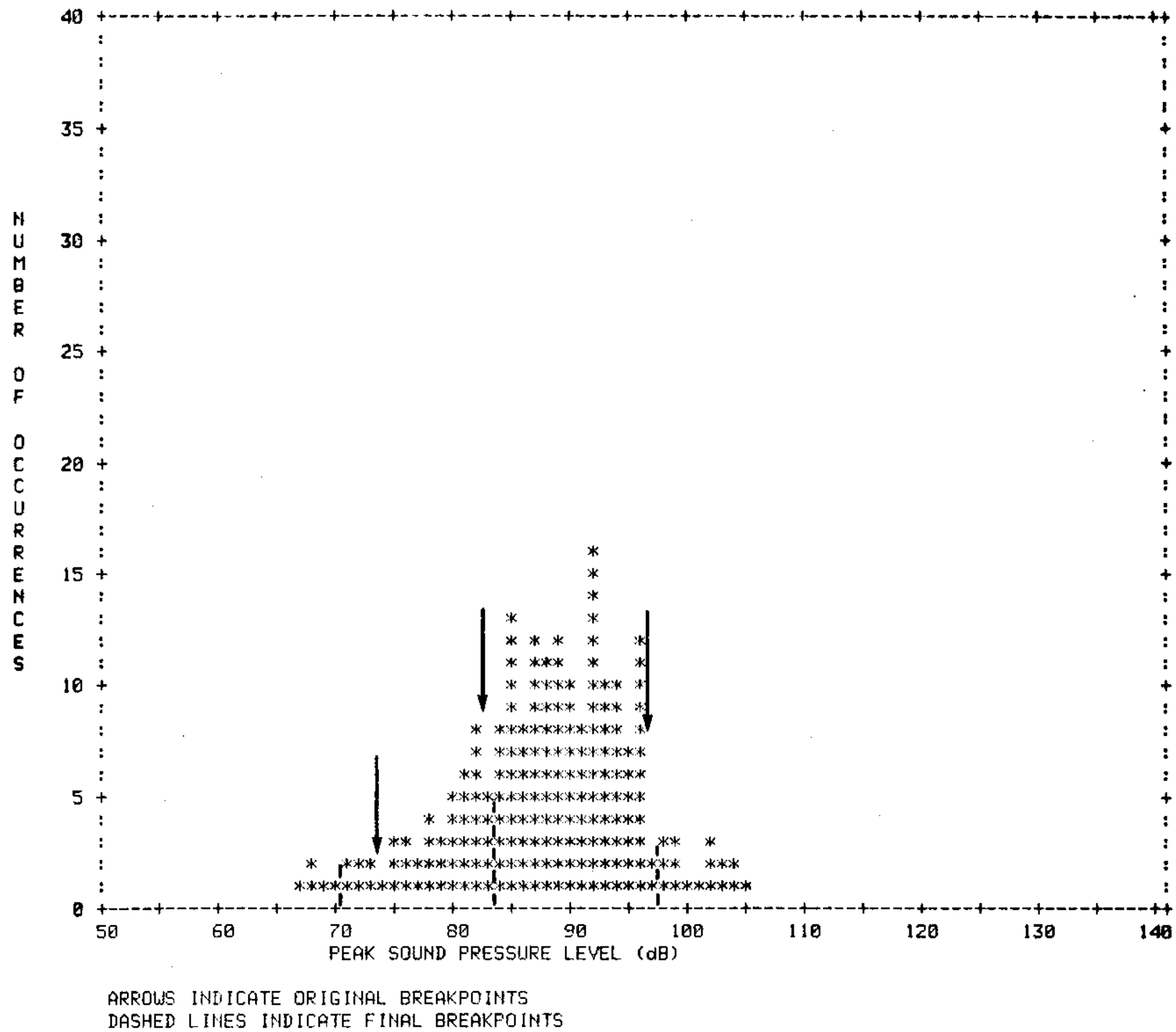

Figure B8. Fifteen-mi daytime peak sound pressure level distribution (original and final breakpoints).

Table B1. Breakpoints in the peak sound pressure level distributions (dB).

Time Period	Distances mi (km)	Ranges 1 & 2 Initial	Ranges 1 & 2 Final	Ranges 2 & 3 Initial	Ranges 2 & 3 Final	Ranges 3 & 4 Initial	Ranges 3 & 4 Final
Night	2 (3)	98	98	109	110	120	120
	5 (8)	80	81	88	94	107	107
	10 (16)	80	77	89	89	100	101
	15 (24)	77	74	85	84	102	98
Day	2 (3)	100	101	110	110	116	120
	5 (8)	80	81	92	96	110	107
	10 (16)	74	74	87	88	100	101
	15 (24)	75	71	83	84	97	98

Initial and Final Breakpoints Between (column group heading for Ranges 1 & 2, 2 & 3, 3 & 4)

Table B2. Extension of ranges in each peak sound pressure level distribution.

Time Period	Distances mi (km)	Extension of Values, dB: Range 1	Range 2	Range 3	Range 4
Night	2 (3)	50-97	98-109	110-119	120-135
	5 (8)	50-80	81-93	94-106	107-135
	10 (16)	50-76	77-88	89-100	101-135
	15 (24)	50-73	74-83	84-97	98-135
Day	2 (3)	50-100	101-109	110-119	120-135
	5 (8)	50-80	81-95	96-106	107-135
	10 (16)	50-73	74-87	88-100	101-135
	15 (24)	50-70	71-83	84-97	98-135

Distribution

Picatinny Arsenal
ATTN: SMUPA-VP3

US Army, Europe
ATTN: AEAEN

Director of Facilities Engineering
APO New York 09827

DARCOM STIT-EUR
APO New York 09710

HQDA (SGRD-EDE)

Chief of Engineers
ATTN: Tech Monitor
ATTN: DAEN-ASI-L (2)
ATTN: DAEN-FEB
ATTN: DAEN-FEP
ATTN: DAEN-FESA
ATTN: FEZ-A
ATTN: DAEN-MCZ-S
ATTN: DAEN-RDL
ATTN: DAEN-PMS (7)
for forwarding to
National Defense Headquarters
Director General of Construction
Ottawa, Ontario K1AOK2
Canada

Canadian Forces Liaison Officer (4)
U.S. Army Mobility Equipment
Research and Development Cmd
Ft Belvoir, VA 22060

Div of Bldg Research
National Research Council
Montreal Road
Ottawa, Ontario, K1AOR6

Airports and Const. Services Dir.
Technical Info Reference Centre
KAOL, Transport Canada Bldg
Place de Ville, Ottawa, Ontario
Canada, K1AON8

Aberdeen Proving Ground, MD 21005
ATTN: AMXHE/J.D. Weisz

Ft Belvoir, VA 22060
ATTN: Kingman Bldg, Library

Ft Monroe, VA 23651
ATTN: ATEN

Ft McPherson, GA 30330
ATTN: AFEN-FEB

USA-WES
ATTN: Library

6th US Army
ATTN: AFKC-LG-C

US Army Engineer District
New York
ATTN: Chief, Design Br
Philadelphia
ATTN: Library
ATTN: Chief, NAPEN-E
Baltimore
ATTN: Chief, Engr Div
Norfolk
ATTN: Chief, NAOEN-D
Huntington
ATTN: Chief, ORHED

US Army Engineer District
Wilmington
ATTN: Chief, SWAEN-D
Savannah
ATTN: Library
ATTN: Chief, SASAS-L
Mobile
ATTN: Chief, SAMEN-D
Memphis
ATTN: Library
Louisville
ATTN: Chief, Engr Div
Detroit
ATTN: Library
St. Paul
ATTN: Chief, ED-D
Rock Island
ATTN: Library
ATTN: Chief, Engr Div
St. Louis
ATTN: Library
ATTN: Chief, ED-D
Kansas City
ATTN: Library (2)
Omaha
ATTN: Chief, Engr Div
New Orleans
ATTN: Library
ATTN: Chief, LMNED-DG
Little Rock
ATTN: Chief, Engr Div
Tulsa
ATTN: Chief, Engr Div
ATTN: Library
Fort Worth
ATTN: Library
ATTN: Chief, SWFED-D
Albuquerque
ATTN: Library
San Francisco
ATTN: Chief, Engr Div
Sacramento
ATTN: Chief, SPKED-D
Far East
ATTN: Chief, Engr Div
Japan
ATTN: Library
Portland
ATTN: Library
Seattle
ATTN: Chief, EN-DB-ST
Walla Walla
ATTN: Library
ATTN: Chief, Engr Div
Alaska
ATTN: Library
ATTN: NPADE-R

US Army Engineer Division
Europe
ATTN: Technical Library
New England
ATTN: Chief, NEDED-T
ATTN: Library
North Atlantic
ATTN: Chief, NADEN-T
Middle East (Rear)
ATTN: MEDED-T
South Atlantic
ATTN: Chief, SADEN-TS
ATTN: Library
Huntsville
ATTN: Library (2)
ATTN: Chief, HNDED-CS
ATTN: Chief, HNDED-SR
Lower Mississippi Valley
ATTN: Library

US Army Engineer Division
Ohio River
ATTN: Chief, Engr Div
ATTN: Library
North Central
ATTN: Library
Missouri River
ATTN: Library (2)
ATTN: Chief, MRDED-T
Southwestern
ATTN: Library
ATTN: Chief, SWDED-T
South Pacific
ATTN: Chief, SPDED-TG
Pacific Ocean
ATTN: Chief, Engr Div
North Pacific
ATTN: Chief, Engr

Facilities Engineers
Ft Campbell, KY 42223
FORSCOM
Ft Devens, MA 01433
Ft Carson, CO 80913
Ft Lewis, WA 98433
USAECOM
Ft Monmouth, NJ 07703
USAIC (2)
Ft Benning, GA 31905
USAAVNC
Ft Rucker, AL 36361
CAC&FL
Ft Leavenworth, KS 66027
USACC
Ft Huachuca, AZ 85613
TRADOC
Ft Monroe, VA 23651
Ft Gordon, GA 30905
Ft Sill, OK 73503
Ft Bliss, TX 79916
HQ, 1st Inf Div & Ft Riley, KS 66442
HQ, 5th Inf Div & Ft Polk, LA 71459
HQ, 7th Inf Div & Ft Ord, CA 93941

AF/PREEU
Bolling AFB, DC 20332

AF Civil Engr Center/XRL
Tyndall AFB, FL 32401

Little Rock AFB
ATTN: 314/DEEE (Mr. Gillham)
Jacksonville, AR 72076

US Naval Oceanographic Office
Wash DC 20373

Naval Air Systems Command
Wash DC 20360

NAVFAC/Code 04
Alexandria, VA 22332

Port Hueneme, CA 93043
ATTN: Library (Code L08A)

Washington, DC
ATTN: Bldg Research Advisory Board
ATTN: Transportation Research Board
ATTN: Library of Congress (2)
ATTN: Dept of Transportation Library

Defense Documentation Center (12)

Engineering Societies Library
New York, NY 10017

U.S. Army Eng District, Ft. Worth
ATTN: Derwood Jones
ATTN: Tom E. Hay
ATTN: Bill G. Daniels
ATTN: Royce W. Mullens,
Water Resource Planning
Environmental Resources Section
P.O. Box 17300
Ft. Worth, TX 76102

DFAE Envir Quality Section
ATTN: Mike Halla
Fort Carson, CO 80192

Commander
Ft. Sill
ATTN: DFAE/D. Hergenrether
Ft. Sill, OK 73503

Human Engr Lab
ATTN: George Garinther
Aberdeen Proving Ground, MD 21005

Director
US Army Engr Waterway Exp Sta
ATTN: Jack Stoll/WESSE
PO Box 631
Vicksburg, MS 39180

HQ US Army Materiel
DARCOM
ATTN: DRCPA-E/E. Proudman
ATTN: J. Pace
501 Eisenhower Ave
Alexandria, VA 22333

US Army Envir Hygiene Agency
ATTN: CPT George Luz/BioAcoustics
Aberdeen Proving Ground, MD 21010

US Training and Doctrine Command
ATTN: ATEN-FE-E/D. Dery
ATTN: James L. Aikin, Jr.
Chief, Environmental Branch
Ft. Monroe, VA 23651

US Army Aeromedical Research Lab
ATTN: Robert T. Camp, Jr.
ATTN: CPT J. Patterson
Box 577
Fort Rucker, AL 36360

Commander
Fort Belvoir
ATTN: Sam Wehr
ATTN: Paul Hopler
System & Components Branch
Ft. Belvoir, VA

US Army Corps of Engineers
South Atlantic Div
ATTN: SDACO-H/B. Alley
510 Title Bldg
30 Pryor St
Atlanta, GA 30303

HQ US Army Forces Command
Office of the Engineer (AFEN-EQ)
ATTN: Robert Montgomery
ATTN: Robert Jarrett
Fort McPherson, GA 30330

US Army Medical Bioengineering
R&D Laboratory
Environmental Protection Research Div
ATTN: LTC LeRoy H. Reuter
Fort Detrick
Frederick MD 21701

Chief of Engineers
ATTN: DAEN-MCE-A/W. B. Holmes
ATTN: DAEN-MCC-E/D. Spivey
ATTN: DAEN-MCC-E/P. Van Parys
ATTN: DAEN-MCE-P/F. P. Beck (2)
ATTN: DAEN-MCE-P/J. Halligan
ATTN: DAEN-ZCE-D/D. M. Benton (2)
Dept of the Army
Wash DC 20314

Director
6570 AMRL/BBE
ATTN: Dr. H. Von Gierke
ATTN: Jerry Speakman
ATTN: LTC D. Johnson, BBA
Wright-Patterson AFB, OH 45433

HQ USAF/PREVX
Pentagon
ATTN: LTC Menker
Wash DC 20330

Nav Undersea Center, Code 401
ATTN: Bob Gales
ATTN: Bob Young
San Diego, CA 92132

Naval Air Station
ATTN: Ray Glass/Code 661
ATTN: Mark Longley-Cook/Code 66102
Building M1
Naval Air Rework
North Island, CA 92135

MAJ Robert Dettling
US AF-ETAC/ENB
Bldg 159
Navy Yard Annex
Wash DC 20333

Naval Facilities Engineering Command
ATTN: David Kurtz
Code 2013C
Hoffman #2
200 Stovall St
Alexandria, Va 22332

Chief of Naval Operations
ATTN: LTJG R. F. Krochalis
200 Stovall St
Alexandria, VA 22332

Federal Aviation Administration
ATTN: Mr. C. Foster/AEQ
ATTN: ARD-530/J. McCullough
ATTN: H.B. Safeer, Chief Envir Policy Div
ATTN: AEQ 200/Dick Tedrick
800 Independence Ave SW
Wash DC 20591

National Bureau of Standards
ATTN: Curtis I. Holmer
ATTN: Dan R. Flynn
ATTN: Arthur I. Rubin
ATTN: Simone Yaniv, Bldg 226, Rm A313
Wash DC 20234

Federal Highway Administration
ATTN: C. Van Bevers
Region 15 Office
1000 N. Glebe Rd
Arlington, VA 22201

Bureau of National Affairs
1231 25th St NW
ATTN: Fred Blosser
Room 462
Wash DC 20037

Office of Noise Abatement
ATTN: Gordon Banerian

Office of the Secretary
400 7th St SW
Wash DC 20590

Department of Housing & Urban Dev
ATTN: George Winzer
Ch. Noise Abatement Program
Office of Res & Tech
Wash DC 20410

NASA
ATTN: H. Hubbard
ATTN: D. Maglieri
ATTN: Dave Hilton
Hampton, VA 23365

EPA Noise Office
ATTN: Al Hicks, Room 2113
John F. Kennedy Federal Bldg
Boston, MA 02203

Environmental Protection Agency
ATTN: George Putnicki
1600 Patterson
Dallas, TX 75201

Environmental Protection Agency
ATTN: Tom O'Hare
Noise Office (Rm 907G)
26 Federal Plaza
New York, NY 10007

EPA Region III Noise Program
ATTN: Pat Anderson
Curtis Bldg, 6th & Walnut
Philadelphia, PA 19106

Environmental Protection Agency
ATTN: AW-471/Cosimo Caccavari
ATTN: AW-471/H. Nozick
ATTN: AW-471/A. Konheim
ATTN: AW-471/L. C. Gray
ATTN: AW-471/J. Shampan
ATTN: R. Marrazzo
ATTN: Fred Mintz, Aircraft Noise
Regulation Officer
ATTN: Basil Manns
ATTN: William Sperry
ATTN: J. Goldstein
ATTN: D. Gray
ATTN: D. Mudarri
Wash DC 20460

Environmental Progection Agency
ATTN: Robert A. Simmons
Rocky Mountain-Prairie Region
Suite 900 Lincoln Bldg
1860 Lincoln St
Denver, CO 80203

EPA Noise Office (Room 109)
ATTN: Dr. Kent Williams
1421 Peachtree St
Atlanta, GA 30309

Illinois Environmental Protection Agency
ATTN: DNPC/Greg Zak
ATTN: Bob Hellweg
ATTN: J. Reid
2200 Churchill Rd
Springfield, IL 62706

Kentucky Department of Labor
ATTN: John Summersett
Div of Educational Training
Frankfort, KY 40601

International Harvester
ATTN: Walter Page
7 South 600 County 1 Mile Rd
Hinsdale, IL 60521

Joiner-Pelton-Rose, Inc.
ATTN: Jack R. Randorff
10110 Monroe Drive
Dallas, TX 75229

Kamperman Associate, Inc.
ATTN: George Kamperman
1110 Hickory Trail
Downers Grove, IL 60515

Paul Borsky
367 Franklin Avenue
Franklin Square, NY 11610

Tom Gutman
1921 Jefferson Davis Hwy
Crystal Mall, Bldg 2
Arlington, VA 20620

Booz-Allen Applied Reseach Div
ATTN: Robert L. Hershey, P.E.
4733 Bethesda Ave
Bethesda, MD 20014

Lee E. Gates
2266 East Rd
Mobile, AL 36609

Green Construction Co.
Charlie E. Sanders, VP
Equipment & Purchasing
1321 Walnut St
Des Moines, IA 50309

Cedar Knolls Acoustical Lab
ATTN: Dick Guernsey
9 Saddle Rd
Cedar Knolls, NJ 07927

Ms. Charolette Rines
1921 Jefferson Davis Hwy
Crystal Mall #2
Room 1105
Arlington, VA 20460

Sensory Sciences Research Ctr
ATTN: Karl Kryter
ATTN: Jim Young
333 Ravenwood Ave
Menlo Park, CA 94025

College of Law
ATTN: Mr. Plager
University of Illinois
Champaign, IL 61820

General Motors Proving Ground
ATTN: Ralph K. Hillquist
Milford, MI 48042

Bolt Beranek & Newman, Inc
ATTN: Kenneth M. Eldred
50 Moulton St
Cambridge, MA 02138

Bolt Beranek & Newman, Inc.
ATTN: Dr. B. Galloway
ATTN: Dr. S. Fidell
ATTN: Dr. Pearsons
21120 Vanowen St
PO Box 633
Canoga Park, CA 91305

Engineering Dynamics, Inc.
ATTN: Robert C. Chanaud
Noise & Vibration
6651 South Wellington Ct
Littleton, CO 80121

Georgia Institute of Technology
Department of City Planning
ATTN: Clifford Bragdon
Atlanta, GA 30083

Dames & Moore
ATTN: Dr. Frederick M. Kessler
6 Commerce Drive
Cranford, NJ 07016

Bonitron, Inc.
ATTN: Robert W. Benson
2670 Sidco Drive
Nashville, TN 37204

Caterpillar Tractor Co.
ATTN: K. Kleimenhagen
Basic Engines Engineering
Bldg W
Mossville, IL 61552

Caterpillar Tractor Co.
ATTN: Les D. Bergsten
ENG-GO, AB 6D
6442 N. Oakbrook Ct
Peoria, IL 61614

Westinghouse Electrical Corp
Research & Development Ctr
ATTN: Jim B. Moreland
Churchill Boro
Pittsburg, PA 14235

Systems Technology Corp
ATTN: Gregor Rigo
245 N. Valley Rd
Xenia, OH 45385

Daniel Queen
5524 Gladys Ave
Chicago, IL 60644

Sandia Corporation
ATTN: Jack Reed
PO Box 5800
Albuquerque, NM 87115

Society of Automotive Engrs
ATTN: William J. Toth
400 Commonwealth Dr
Warrendale, PA 15096

Wyle Labs
ATTN: L. Sutherland
128 Maryland St
El Segundo, CA 90245

Consolidated Edison Co., of NY
ATTN: Allan Teplitzky
4 Irving Plaza
New York, NY 10003

Pennsylvania State University
101 Engineering A Bldg
University Park, PA 16802

Construction and Industrial Machinery
ATTN: J. Arndt
Production Safety Dept
Moline, IL 61265

Donaldson Co.
ATTN: S. Schmeichel
PO Box 1299
Minneapolis, MN 55440